Persistent acetylation of newly synthesized histones inhibits DNA replication origin activity

Roch Tremblay[1,2], Yosra Mehrjoo[1,2], Antoine Simoneau[1,2], Mary McQuaid[1], Corey Nislow[4], Guri Giaever[4], Hugo Wurtele[1,3*]

1. Centre de recherche de l'Hôpital Maisonneuve-Rosemont, 5415 boulevard de l'Assomption, Montréal, H1T 2M4, Canada

2. Molecular Biology Program, Université de Montréal, 2900 Édouard-Montpetit, Montréal, Québec, Canada, H3T 1J4

3. Department of Medicine, Université de Montréal, 2900 Édouard-Montpetit, Montréal, Québec, Canada, H3T 1J4

4. Department of Pharmaceutical Sciences, University of British Columbia, Vancouver, Canada

* Corresponding author

Email: hugo.wurtele@umontreal.ca

ABSTRACT

Histone acetylation is a known regulator of DNA replication dynamics. In the yeast *Saccharomyces cerevisiae*, newly synthesized histone H3 deposited behind DNA replication forks are acetylated on lysine 56 (H3 K56ac) by the Rtt109 histone acetyltransferase. Two enzymes of the sirtuin family of deacetylases, Hst3 and Hst4, act redundantly to deacetylate this residue throughout chromosomes following S phase. Cells lacking Hst3 and Hst4 present constitutively acetylated H3 K56, which causes sensitivity to replication-blocking genotoxins and slow growth via mechanisms that remain poorly understood. Here, we present the results of a genome-wide screen aimed at identifying haploinsufficient genes that promote cell fitness in response to inhibition of sirtuins by nicotinamide (NAM). We find that heterozygous deletion alleles of genes involved in the regulation of DNA replication origins sensitize cells to NAM. Consistently, haploid cells harboring the hypomorphic temperature sensitive allele *cdc7-4* present striking NAM-induced S phase progression defects at their semi-permissive temperature. We further show i) that Rap1-interacting factor 1 (Rif1), an inhibitor of Cdc7-dependent activation of replication origins, causes DNA damage and replication defects in cells exposed to NAM and in *hst3*Δ *hst4*Δ mutants, and ii) that *cdc7-4 hst3*Δ *hst4*Δ triple mutant cells present strong synthetic temperature sensitivity associated with defective activation of replication origin and delayed S phase progression. Our data further demonstrate that such replication defects are not due to intra-S phase checkpoint activation leading to inhibition of origin activity. We finally show that Rtt109-dependent acetylation of histone H3 lysine 56 and its associated Rtt101-Mms1 ubiquitin ligase complex cause the DNA replication defects observed in *cdc7-4 hst3*Δ *hst4*Δ cells. Overall, these results argue that abnormal regulation of nascent chromatin structure negatively influences DNA replication initiation in cells presenting reduced Dbf4-dependent kinase activity including those experiencing replicative stress.

INTRODUCTION

DNA replication initiates at multiple origins throughout chromosomes during the S phase of the cell cycle [1]. During G1, Cdt1 and Cdc6 load the MCM helicase complex on DNA at origins of replication bound by the Origin Recognition Complex (ORC). At the beginning of S phase, cyclin-dependent (CDK) and Dbf4-dependent (DDK) kinase activities promote the recruitment of other factors including Cdc45 and the GINS complex to replication origins as well as the activation of the MCM helicase. Melting of origin DNA resulting from MCM helicase activity allows the formation of two replication forks (RF) that travel in opposite directions along chromosomal DNA. Depending on the timing of their activation in S phase, eukaryotic origins are classified as early, mid, or late. Such sequential activation of origins has been shown to result from the recycling of limiting replication initiation factors from early to mid, and then to late replicating genomic regions[2,3]. While the above-described temporal organization of DNA replication is evolutionarily conserved among eukaryotes, its functional relevance is incompletely understood.

RF progression can be halted upon encountering DNA lesions induced by any among a multitude of environmental or endogenous genotoxins [4]. This engenders a state of replicative stress which can forestall completion of chromosomal duplication, thereby causing genomic instability. Stalled RF cause the activation of Mec1 (ATR in humans), the apical kinase of the intra-S phase checkpoint response in yeast [4]. Mec1 then promotes activation of the kinase Rad53 via one of two pathways dependent upon either the RF component Mrc1 or the adaptor Rad9 [5]. Mec1 and Rad53 subsequently phosphorylate a multitude of substrates to i) promote the stability of stalled RF, and ii) to prevent further activation of replication origins [6]. In yeast, this latter effect depends on Rad53-dependent phosphorylation of the key replication factors Dbf4 and Sld3, which prevents the activation of the MCM helicase at origins that have not yet fired [7]. Such inhibition of origin activity is thought to prevent the accumulation and eventual collapse of stalled RF during periods of genotoxic stress [8].

Histone post-translational modifications are critical determinants of DNA replication dynamics and origin activity [9,10]. Of interest here, histone lysine acetylation has been shown to both promote and inhibit origin activity depending on the identity of the modified residue and/or chromosomal context [11]. The sirtuin family of histone deacetylases is well-conserved throughout evolution, and several of its members influence DNA replication and repair [12]. The yeast

Saccharomyces cerevisiae possesses 5 sirtuins; the founding member, Sir2, and Homologues of Sir Two 1 through 4 (Hst1-4) [12]. Sir2 targets histone H4 lysine 16 acetylation (H4 K16ac) thereby repressing the firing of origins at the rDNA locus and telomeres [13,14]. Hst1, which can also target H4 K16ac, forms a complex with Sum1 and Rfm1 and positively regulates a subset of origins genome-wide [15,16]. While the impact of Hst2 on DNA replication has not been directly assessed, at least some of the functions of this sirtuin are known to be partially redundant with those of Sir2, as overexpressed Hst2 rescues gene silencing defects caused by *sir2*Δ [17,18].

The only known histone substrate of the redundant sirtuins Hst3 and Hst4 is acetylated H3 lysine 56 (H3 K56ac) [19]. This modification is catalysed by the acetyltransferase Rtt109 on newly synthesized histones H3 before their deposition onto nascent DNA during S-phase [20,21]. After completion of DNA replication, Hst3 and Hst4 remove H3 K56ac chromosome-wide such that most nucleosomes do not harbor H3 K56ac at the start of the next S phase. While under normal circumstances the bulk of H3 K56ac is removed by Hst3 during G2, Hst4 can compensate for its absence. As such, the stoichiometry of H3 K56ac approaches 100% throughout the cell cycle in *hst3*Δ *hst4*Δ double mutants [19,22]. Such constitutive H3 K56ac has been shown to cause spontaneous DNA damage, thermosensitivity, and increased sensitivity to genotoxins that cause replicative stress [19,23,24]. However, the molecular mechanisms underlying the striking phenotypes of *hst3*Δ *hst4*Δ cells remain poorly understood.

Nicotinamide (NAM) is a non-competitive pan-inhibitor of sirtuins [25]. Our group previously performed genetic screens in *S. cerevisiae* with the goal of identifying genes whose homozygous deletion (i.e. complete loss-of-function) confers either fitness defects or advantages in response to NAM-induced sirtuin inhibition and consequent H3 K56 hyperacetylation [26]. These screens revealed that genes encoding regulators of the DNA replication stress response promote resistance to NAM-induced elevation in H3 K56ac caused by inhibition of Hst3 and Hst4 [26,27]. While the mechanisms are unclear, previous data indicate that cells lacking HST3 are defective in the maintenance of artificial chromosomes harboring a reduced number of DNA replication origins [28], further linking H3 K56ac with regulation of DNA replication dynamics. Here, we present the results of a genome-wide haploinsufficiency screen aimed at identifying genes modulating cell fitness in response to NAM-induced sirtuin inhibition. Overall, our results indicate that i) factors promoting DNA replication origin activation are critical for survival in the

absence of Hst3 and Hst4 activity, and ii) abnormal persistence of the acetylation of new histones deposited into chromatin during S phase compromises the activity of replication origins in yeast.

RESULTS

A genetic screen to identify genes modulating cellular fitness in response to NAM.

We performed a screen using the pooled strains of the heterozygote diploid yeast collection to identify haploinsufficient genes that affect cell fitness upon NAM-induced inhibition of sirtuins (Supplementary Table 1). Using a Z-score cut-off of +/- 2.58 (99% cumulative percentage), the screen identified 131 and 58 genes whose heterozygosity caused reduced or increased fitness, respectively, during propagation for 20 generations in YPD medium containing 41 mM NAM (Figure 1A). This list of genes presents only modest overlap with that obtained from our previously published screen using the homozygote deletion strain collection (Figure 1B), suggesting that most of the genes identified in the latter screen are not haploinsufficient with regards to NAM sensitivity. This lack of overlap between screens performed on the homozygous and heterozygous deletion collections is consistent with our previous observations [29]. Gene Ontology (GO) term analysis of genes whose heterozygosity sensitizes cells to NAM revealed an obvious enrichment in DNA replication and DNA damage response pathway, whereas terms reflecting proteasome-related and catabolic processes were associated with mutations promoting enhanced fitness upon NAM exposure (Figure 1C and Supplementary Tables 2-3).

We next sought to validate individual heterozygous mutations representing the main categories of “hits” identified in the screen. In these two-strains competitions, WT and heterozygote diploid mutant strains of interest were mixed in a 1:1 ratio and incubated for 20 generations in YPD +/- NAM. Appropriate dilutions of cells were then plated on YPD-agar +/- G418 and the ratio of the number of heterozygote mutant (G418-resistant) vs WT (G418-sensitive) colonies was calculated (Figure 1D). This competition analysis confirmed the expected impact of heterozygous mutation causing diminished cell fitness in NAM-containing medium, thereby validating our screening strategy. In contrast, significant improvement in growth was not observed for individual heterozygote mutants expected to elevate fitness (Supplementary Figure 1). We note that heterozygote mutations causing improved fitness in response to NAM displayed generally

lower absolute Z-scores than those reducing fitness (Figure 1A, Supplementary Table 1). This may reflect modest differences in growth that might be challenging to detect in 1:1 vs genome-wide competition. In view of the above considerations, we decided to focus on further characterization of genes whose heterozygosity reduced cell fitness in response to NAM.

Deregulation of DNA replication origin activity sensitizes cells to NAM

As mentioned previously, cells lacking Hst3 are defective in the maintenance of an artificial chromosome harboring reduced number of DNA replication origins, revealing a potential link between this sirtuin and origin activity whose mechanistic basis is unknown [28]. Interestingly, several essential DNA replication genes identified in the screen as promoting NAM resistance are involved in the assembly of the pre-replication complex (*ORC3*, *ORC5*, *CDC6* and *MCM4*) or regulation of origins activation (*CDC7*, *DBF4*, *SLD3* and *GLC7*). We chose to focus on the relationship between NAM sensitivity and the role of Cdc7-Dbf4 (DDK) in promoting origin activation. Consistent with results from the screen, haploid cells expressing hypomorphic temperature sensitive alleles of *DBF4* (*dbf4-1*) and *CDC7* (*cdc7-4*) are sensitized to NAM when incubated at the semi-permissive temperature of 30°C (Figure 2A). Our data also indicate that *bob1-1 cdc7*Δ cells, which harbor a mutation in MCM5 that bypasses DDK-dependent MCM phosphorylation for origin activation [30], are not NAM-sensitive (Figure 2B), arguing that the MCM complex is likely to be the relevant target of DDK in this context. Overall, these results suggest that impaired activation of DNA replication origins sensitizes cells to NAM.

Rap1-Interacting Factor 1 (Rif1) acts in concert with the phosphatase Glc7 to reverse DDK-dependent MCM phosphorylation, thereby inhibiting origin activation [31–34]. Moreover, a previous screen performed by our group identified *RIF1* among the few yeast genes whose homozygous deletion improved cell fitness in NAM-containing medium [26]. Interestingly, we found that NAM-induced growth defects and accumulation of cells in S phase is rescued by deletion of *RIF1* (Figure 2C and G). Moreover N-terminal truncation or mutations in the Glc7-interacting motif (*rif1*-RVxF/SILK) of Rif1, both of which were previously shown to partially suppress the temperature sensitivity of *cdc7-4* mutants by eliminating Rif1 binding to Glc7 [33,35], also strongly suppressed the NAM sensitivity of *cdc7-4* cells (Figure 2C). Overall, these data are

consistent with the notion that Rif1/Glc7-dependent dephosphorylation sensitizes cells with reduced DDK activity to NAM.

We and others previously showed that NAM treatment causes replicative stress and DNA damage in yeast [19,26,27]. Since lack of MCM phosphorylation by DDK causes sensitivity to replicative stress-inducing drugs [36,37], we tested the impact of *RIF1* deletion on NAM-induced DNA damage. Compared to WT, *rif1*Δ cells presented reduced NAM-induced histone H2A S129 phosphorylation and Rad52-YFP foci formation (Figure 2D-E), two well-known markers of replicative stress-induced DNA damage [38,39]. Importantly, lack of Rif1 did not compromise the formation of ionizing radiation (IR)-induced Rad52 foci, which are not primarily caused by replication-associated DNA damage. We note that, in addition to its role in regulating DNA replication, Rif1 is known to limit telomere length by inhibiting telomerase activity [40]. Since we previously showed that cells with short telomeres are sensitive to NAM-induced sirtuin inhibition [27], we considered the possibility that abnormal telomere elongation in *rif1*Δ cells might favor NAM resistance. Contrary to this notion, deletion of *RIF1* suppressed NAM-induced growth and S phase progression defects in telomerase-defective *est2*Δ cells (Figure 2F), indicating that the role of Rif1 in modulating NAM sensitivity is independent of its influence on telomere length.

Lack of Hst3/Hst4 activity inhibits the initiation of DNA replication in *cdc7-4* cells in a Rif1-dependent manner

We previously showed that NAM-induced DNA damage is attributable to inhibition of H3 K56ac deacetylation by Hst3 and Hst4 [26]. We therefore tested the impact of Rif1 on the phenotypes caused by lack of *HST3* and *HST4*. We found that deletion of *RIF1* rescues the temperature sensitivity of *hst3*Δ *hst4*Δ cells as well as the synthetic lethality of *hst3*Δ *hst4*Δ *sir2*Δ without affecting the levels of H3 K56ac (Figure 3A-B). We note that for unknown reasons *hst3*Δ *hst4*Δ cells are only temperature sensitive in S288C-derived genetic backgrounds and not in W303 (our unpublished observations; e.g., compare Figure 3A and 3G). Because of this, while most of the experiments involving *hst3*Δ *hst4*Δ were done in W303-derived strains, certain experiments including the one presented in Figure 3A were done in the BY4741 background (see Supplementary Table 4 for a description of the yeast strains used in each figure of this study).

We previously demonstrated that transient exposure to methyl methane sulfonate, an alkylating agent that generates DNA replication blocking lesions such as 3-methyl adenine, prevents timely completion of S phase in *hst3*Δ *hst4*Δ cells [24]. DNA content flow cytometry analyses revealed that deletion of *RIF1* noticeably rescued the S phase progression delay caused by transient MMS exposure in *hst3*Δ *hst4*Δ double mutants (Figure 3C), consistent with the notion that Rif1 compromises DNA replication completion in these cells. Nevertheless, deletion of *RIF1* did not rescue the sensitivity of *hst3*Δ *hst4*Δ to MMS (Figure 3D), which is possibly due to the fact that Rif positively modulates the stability of stalled RF [41]. We also found that *rif1*Δ reduced spontaneous formation of Rad52 foci and histone H2A S129 phosphorylation in *hst3*Δ *hst4*Δ cells (Figure 3E-F), indicating that, in the absence of exogenous replicative stress-inducing genotoxins, Rif1 activity causes DNA damage in Hst3/Hst4-deficient cells. The above data suggest that Rif1/Glc7-mediated reversal of DDK-dependent phosphorylation, and consequent inhibition of origins of DNA replication, contribute to the phenotypes of cells lacking Hst3 and Hst4. Consistent with this idea, deletion of *HST3* and *HST4* considerably exacerbated the temperature sensitivity of *cdc7-4* mutant cells in a Rif1-dependent manner (Figure 3G), and *rif1*Δ diminished H2A S129 phosphorylation in *cdc7-4 hst3*Δ *hst4*Δ mutants (Figure 3F). Deletion of either *HST3* or *HST4* alone did not increase the temperature sensitivity of *cdc7-4* (Figure 3H), in accord with the known functional redundancy of Hst3/4 with respects to histone deacetylation [19,22].

We next evaluated DNA replication dynamics in *cdc7-4* cells lacking Hst3/Hst4. *cdc7-4 hst3*Δ *hst4*Δ cells displayed strong Rif1-dependent S phase progression inhibition at the semi-permissive temperature of 30°C compared to either *hst3Δ hst4Δ* or *cdc7-4* (Figure 4A). As expected, this phenotype was rescued by deletion of *RIF1* (Figure 4A) or expression of plasmid-borne copy of *HST3* (Figure 4B). The observed DNA replication defect does not appear to result from compromised release from alpha factor-mediated G1 arrest, since asynchronously growing *cdc7-4 hst3*Δ *hst4*Δ cells accumulated in early S when incubated at 30°C (Figure 4C). Moreover, the budding index of *cdc7-4 hst3*Δ *hst4*Δ cells released from alpha factor-mediated G1 block toward S phase at 30°C was comparable to that of *cdc7-4* cells (≈80%) even though the former cells present barely detectable S phase progression (Figure 4D-E). The above data indicate that *cdc7-4 hst3*Δ *hst4*Δ can enter S phase at the semi-permissive temperature but fail to synthesize DNA efficiently.

The very limited extent of DNA synthesis observed in *cdc7-4 hst3*Δ *hst4*Δ vs *cdc7-4* cells raised the possibility that activation of early replication origins might be compromised in the absence of Hst3 and Hst4. Using quantitative PCR, we found that, compared to *cdc7-4* mutants, duplication of DNA was inhibited at multiple early origins in *cdc7-4 hst3*Δ *hst4*Δ vs *cdc7-4* cells 30 minutes after release from alpha factor arrest at 30°C (Figure 4F). This represents a strong delay in origin activation rather than permanent inhibition since *cdc7-4 hst3*Δ *hst4*Δ cells eventually initiate replication and complete S phase when incubated for longer periods at 30°C (240 minutes post-release from alpha factor arrest; Figure 4G-H). To independently confirm the above results, we used a previously described method based on alkaline gel electrophoresis and southern blotting to detect nascent DNA formation at the efficient early origin ARS305 [6]. Strikingly, the results indicate that minimal nascent DNA was formed at this origin within 1 h of release from alpha factor arrest at 30°C in *cdc7-4 hst3*Δ *hst4*Δ cells when compared to *cdc7-4* mutants (Figure 4I). Taken together, the results reveal that lack of Hst3/4 activity compromises the activation of origins of replication in cells presenting reduced DDK activity.

Inhibition of origin activity is not due to intra S phase checkpoint activation in *cdc7-4 hst3*Δ *hst4*Δ cells

One of the key roles of intra S phase checkpoint signalling is to limit the activation of origins in response to replication stress [6,42], which occurs in part via negative regulation of DDK activity depending on the phosphorylation of Dbf4 by Rad53 [7]. Cells lacking Hst3/4 activity are well-known to present spontaneous DNA damage and constitutive activation of Rad53 [19,23,24,26,27]. We therefore sought to evaluate if the striking S phase progression delay observed in *cdc7-4 hst3*Δ *hst4*Δ cells is caused by elevated Rad53 activation at the semi-permissive temperature of *cdc7-4* (30°C). While *cdc7-4 hst3*Δ *hst4*Δ cells constitutively present some Rad53 phosphorylation, no detectable elevation in Rad53 phosphorylation-induced electrophoretic mobility shift was observed upon release of cells from alpha factor arrest toward S phase at 30°C, either in the presence or absence of the replication-blocking genotoxin hydroxyurea (HU; Figure 5A-B). This result is consistent with the notion that few if any RF are progressing in these conditions (Figure 4F, I). This, in turn, is expected to reduce the number of stalled replication forks

in either HU-treated or untreated conditions thereby compromising the activation of intra S phase checkpoint kinases.

Mrc1 and Rad9 are key mediators of intra S phase checkpoint activation [5]. We found that deletion of *RAD9* led to modestly increased S phase progression, but only at later time points, in *cdc7-4 hst3*Δ *hst4*Δ cells (Figure 5C). This suggests that Rad9 might contribute to the maintenance rather that the establishment of the replication defects observed in *cdc7-4 hst3*Δ *hst4*Δ cells over longer time periods. In contrast, expression of a mutated allele of Mrc1 (Mrc1-AQ) which compromises its role in the intra S phase checkpoint [43] does not detectably improved S phase progression in *cdc7-4 hst3*Δ *hst4*Δ cells even at later time points (Figure 5D). We further found that inhibition of Mec using caffeine [44,45] completely abrogated Rad53 phosphorylation, as expected, but did not reverse the strong inhibition of DNA replication progression of *cdc7-4 hst3*Δ *hst4*Δ mutants (Figure 5E-F). Importantly, caffeine exposure did not prevent *cdc7-4* cells from completing DNA replication at 30°C (Figure 5F). Expression of Dbf4 and Sld3 variants that cannot be phosphorylated by Rad53 was previously shown to abrogate intra S phase checkpoint-dependent inhibition of origin activity in yeast [7]. We found that introducing such mutated alleles of *DBF4* and *SLD3* in *cdc7-4 hst3*Δ *hst4*Δ cells does not alleviate their S phase progression defects at 30°C (Figure 5G). Taken together, the data argue that intra S phase checkpoint activity does not underlie the incapacity of *cdc7-4 hst3*Δ *hst4*Δ mutants to initiate DNA replication in a timely manner when incubated at the semi-permissive temperature for *cdc7-4*.

Constitutive histone H3 lysine 56 acetylation causes replication defects in *cdc7-4* cells

Constitutive acetylation of histone H3 lysine 56 (H3 K56ac) was previously shown to cause most of the phenotypes associated with *hst3*Δ *hst4*Δ mutants, including their temperature and DNA damage sensitivity [19,22,23]. H3 K56ac strictly depends on the Rtt109 histone acetyltransferase [46]. We found that deletion of *RTT109* rescued DNA replication progression and growth of *cdc7-4 hst3*Δ *hst4*Δ cells at semi-permissive temperatures for *cdc7-4* (between 28°C and 30°C; Figure 6A-C). We next sought to directly implicate H3 K56ac in the phenotypes of *cdc7-4 hst3*Δ *hst4*Δ cells by expressing mutant histone H3 in which lysine 56 has been replaced by a non-acetylable arginine residue (H3 K56R). We tried to engineer appropriate histone mutant strains by deleting both copies of the genes encoding histone H3 (*HHT1* and *HHT2*) and expressing one copy of the

HHT1 gene with or without a mutation resulting in expression of the H3 K56R variant. We failed to generate either an H3 WT- or H3 K56R-expressing *cdc7-4 hst3*Δ *hst4*Δ strain using the standard method described above, suggesting that abnormal histone gene copy number may be lethal in *cdc7-4 hst3*Δ *hst4*Δ cells. We therefore replaced only *HHT1* by either WT or K56R alleles and left the endogenous copy of HHT2 intact to reduce H3 K56ac levels without changing histone gene dosage (Figure 6D-E). This strategy produced viable *cdc7-4 hst3*Δ *hst4*Δ strains in which H3 K56ac is either unchanged or noticeably reduced (Figure 6D-E). Strikingly, we observed a strong rescue of the temperature sensitivity of *cdc7-4 hst3*Δ *hst4*Δ upon expression of H3 K56R (compared to control cells expressing a WT version of H3; Figure 6D). Taken together, the above results indicate that constitutive Rtt109-dependent H3 K56ac inhibits growth and DNA replication in *cdc7-4 hst3*Δ *hst4*Δ cells.

Genetic and biochemical data indicate that Rtt109 and H3K56ac act at least in part by modulating the activity of a ubiquitin ligase complex composed of the Rtt101, Mms1 and Mms22 subunits [47–50]. Indeed, deletion of the genes encoding subunits of this complex is known to partially suppress the phenotypes of *hst3*Δ *hst4*Δ cells [47], although the precise mechanisms linking constitutive acetylation of nucleosomal H3 K56ac and the Rtt101/Mms1/Mms22 complex remain elusive. We found that deletion of either *RTT101* or *MMS1* suppresses the synthetic temperature sensitivity of *cdc7-4 hst3*Δ *hst4*Δ mutant cells. We were unable to generate *cdc7-4 hst3*Δ *hst4*Δ *mms22*Δ cells, suggesting that yet to be determined synthetic interactions between these loci prevent viability. Nevertheless, our results implicate Rtt101-Mms1-containing complexes in H3 K56ac-dependent modulation of DNA replication origin dynamics.

DISCUSSION

New histones are acetylated on several lysine residues which promotes efficient assembly of nucleosomes on replicated DNA [51–53]. In yeast, virtually all new histones H3 are acetylated on K56, leading to a genome-wide wave of histone acetylation at this residue during S phase [19,46]. H3 K56ac promotes timely formation of new nucleosomes by favoring the interaction of new histones with the chromatin assembly factors CAF1 and Rtt106 [51]. While this “pre-deposition” function of H3 K56ac in nucleosome assembly is well-established, several observations indicate that H3 K56ac plays other biological roles following its incorporation into chromatin. Indeed, lack

of nucleosomal H3 K56ac deacetylation in *hst3*Δ *hst4*Δ cells causes sensitivity to replication-blocking drugs and poor growth, suggesting that chromatin-associated H3 K56ac influences the cellular response to replicative stress [22,23]. Moreover, cells have evolved elaborate mechanisms to degrade Hst3 in response to genotoxin exposure during S phase [54,55], suggesting that the ensuing persistence of H3 K56ac may somehow be beneficial to the DNA damage response. Nevertheless, while several cellular pathways have been genetically linked to nucleosomal H3 K56ac [23,24,26,27,47], the molecular basis of the sensitivity of *hst3*Δ *hst4*Δ mutants to replicative stress, as well as the role of H3 K56ac persistence after DNA damage, remain poorly understood.

We previously showed that NAM elevates H3K56ac, thereby causing DNA damage and replicative stress similar to the situation observed for *hst3*Δ *hst4*Δ cells [26]. In accord with this, the screen presented here reveals that a large proportion of genes whose heterozygous inactivation confer NAM sensitivity participate in DNA replication. Our data further indicate that i) reduced activity of Cdc7 and Dbf4 causes growth defects in the presence of NAM, and ii) firing of early/efficient origins of DNA replication is strongly diminished in *cdc7-4 hst3*Δ *hst4*Δ cells at the semi-permissive temperature for *cdc7-4*. Deletion of *RIF1* suppressed the inability of *cdc7-4 hst3*Δ *hst4*Δ to initiate replication and grow at the semi-permissive temperature of *cdc7-4*, in accord with the known role of Rif1 in promoting Glc7-dependent dephosphorylation of MCM complexes thereby inhibiting origin activation [33]. Moreover, lack of Rif1 also suppressed NAM-induced DNA damage, as well as the temperature sensitivity, spontaneous DNA damage, and elevated frequency of Rad52 foci in *hst3*Δ *hst4*Δ cells. Finally, we note that homozygous deletion of *RIF1* was found to confer improved fitness in response to NAM in our previously published screen [26]. The above data are intriguing in light of the fact that Rif1 has been reported to promote the stability of stalled RF [41], which suggests that the contribution of limited origin activity to the phenotypes caused by elevated H3 K56ac overrides the negative impact of *rif1*Δ on replicative stress responses. We also note that published reports indicating that cells lacking Hst3 are unable to maintain a yeast chromosome harboring a reduced number of replication origins, which supports the notion that elevated H3 K56ac negatively influences the ability of cells to replicate their chromosomes under conditions where the number of active origins is limited [28,56].

It is now well-known that histone acetylation and chromatin structure influences DNA replication origin firing efficacy and timing of activation during S phase [10,57]. For example,

cells lacking the histone deacetylase Sir2 exhibit elevated origin activation at the ribosomal DNA locus and in subtelomeric regions [13,58]. Targeting the GCN5 acetyltransferase to an origin was also shown to favor its activation, while deletion of the Rpd3 deacetylase caused late origins to fire earlier in S phase [59]. While in the above-mentioned examples hyperacetylation was shown to promote origin activity, in contrast to hyperacetylation of H3 K56ac, elevated histone acetylation has also been reported to exert a negative influence on origin activity. For example, Sir2 and Rpd3 had opposite effects on the activation of origins located within the rDNA array [11], clearly indicating that histone acetylation can either promote or inhibit origin activity depending on chromosomal context.

RF stalling activates the kinases Mec1 and Rad53, which then phosphorylate a multitude of substrates to effect the various roles of the intra-S phase checkpoint [60]. Rad53 phosphorylates the replication proteins Dbf4 and Sld3 to inhibit the firing of replication origins which have not yet been activated [7]. In apparent contrast to our results, a previously published report revealed that *hst3*Δ *hst4*Δ cells present elevated activation of late origins in cells released from G1 toward S phase in medium containing the replication-blocking ribonucleotide reductase inhibitor HU [11]. However, this was not specific to *hst3*Δ *hst4*Δ cells; indeed, such effect was found to be an indirect consequence of elevated spontaneous DNA damage and constitutive Rad53 activity in various replicative stress response mutants, leading to Rad53-dependent elevation of dNTP pools and consequent HU-resistant DNA replication progression [61]. On the other hand, several observations presented here indicate that constitutive H3 K56ac can influence origin firing in a Rad53-independent manner. First, *cdc7-4 hst3*Δ *hst4*Δ cells do not display elevated Rad53 phosphorylation when released from G1 arrest toward S phase at the semi-permissive temperature for *cdc7-4*. Secondly, mutations or treatments that compromise Rad53 activation, or the ability of this kinase to phosphorylate Sld3 and Dbf4, do not rescue defective initiation of replication in *cdc7-4 hst3*Δ *hst4*Δ mutants. Taken together, the above data argue that the impact of constitutive H3 K56ac on origin activity does not require prior replication fork stalling and ensuing Rad53 activity, and that this histone modification can act before widespread initiation of replication origins in early S phase.

While our data argue that elevated H3 K56ac inhibits DNA replication initiation in a Rad53-independent manner, our results indicate that it does so only under conditions that reduce

DDK activity. Paradoxically, such conditions are met upon activation of the intra S phase checkpoint response; it is therefore expected that H3 K56ac-dependent inhibition of origins would contribute to S phase progression defects in *hst3*Δ *hst4*Δ cells only once RF emanating from early origins have been stalled, leading to Rad53 activation and consequent reduction of DDK activity. In other words, constitutive H3 K56ac and Rad53 activation are expected to act synergistically to inhibit late origin firing during genotoxic stress, thus interfering with the ability of cells to complete DNA replication. Consistent with this notion, we and others previously showed that i) *hst3*Δ *hst4*Δ cells cannot complete DNA replication in a timely manner after transient exposure to genotoxic drugs during S phase [24], ii) *hst3*Δ *hst4*Δ cells present strong and persistent activation of Rad53 upon DNA damage [23,24,26], iii) limiting Rad53 activation partially rescues the phenotypes of *hst3*Δ *hst4*Δ mutants [23,24,26,62], and iv) elevating the firing of late origins of replication by overexpression of Cdc45, Sld3 and Sld7 can rescue certain phenotypes caused by constitutive H3 K56ac [27,62]. Our data also show that deletion of *RAD9* partially rescues defective S phase progression in *cdc7-4 hst3*Δ *hst4*Δ cells, but only at later time points. It is plausible that eventual initiation of a limited number of RF may cause spontaneous activation of Rad53 under these conditions, which in turn might maintain S phase progression defects caused by constitutive H3 K56ac over long periods of time. The combined negative effects of Rad53 activation and elevated H3 K56ac on origin activity is expected to force RF to travel unusually long distances before encountering a converging fork. Consequently, a substantial fraction of persistently stalled RF will not be “rescued” by converging forks, leading to under-replicated chromosomal regions, RF collapse, DNA damage, and eventual arrest in G2/M, which are all observed in *hst3*Δ *hst4*Δ cells [12,19,23,24].

The mechanism linking H3 K56ac to origin activity is currently unknown. As mentioned previously, Mec1 activation promotes degradation of Hst3, which causes H3 K56ac to persist during late S and G2 [54,55]. It is possible that such persistence might contribute to Mec1- and Rad53-dependent inhibition of replication origins. Interestingly, we demonstrated that deletion of *RTT101* or *MMS1*, which encode subunits of a ubiquitin ligase complex previously genetically linked to H3 K56ac [47,48], rescues the synthetic temperature sensitivity of *hst3*Δ *hst4*Δ *cdc7-4*. Since deletion of either *RTT101* or *MMS1* does not influence H3 K56ac levels [47], it is likely that the effect of H3 K56ac is not strictly dependent on modulation of chromatin structure at origins. Rtt101 recruitment to chromatin upon DNA damage was shown to depend at least partly on the

H3 K56 acetyltransferase Rtt109 [50]. Moreover, Mms1 has been reported to interact directly with the Origin Recognition Complex subunit Orc5 [63], although the biological relevance of this interaction is unclear. The above considerations raise the possibility that DNA damage-induced persistence of H3 K56ac might modulate Rtt101/Mms1 activity, leading to regulation of Orc5-bound origins. Further experiments will be required to test the validity of such model, and to precisely ascertain the mechanistic basis of the impact of H3 K56ac on DNA replication dynamics.

ACKNOWLEDGEMENTS

H. W. is the recipient of a Chercheur-boursier Sénior scholarship from Fonds de la Recherche du Québec-Santé (award #281795; https://frq.gouv.qc.ca). This work was supported by Natural Sciences and Engineering Research Council of Canada Discovery Grant and Discovery Accelerator Supplement (RGPIN-2019-05082, RGPAS-2019-00009; https://www.nserc-crsng.gc.ca) and by a Fonds de la Recherche du Québec-Nature et Technologies grant (2018-PR-206098; https://frq.gouv.qc.ca) to H.W. C. N. is supported by the Canadian Foundation for Innovation (CFI; https://www.innovation.ca/) and is a Canada Research Chairs (CRC; https://www.chairs-chaires.gc.ca/) Tier 1 Chair. The funders had no role in study design, data collection and analysis, decision to publish, or preparation of the manuscript. We thank Dr David Shore (Université de Genève) for providing yeast strains, Dr Alain Verreault (Université de Montréal) for the generous gift of anti-H3K56ac and anti-H2A S129-P antibodies, and Dr Elliot A. Drobetsky (Université de Montréal) for critical reading of the manuscript.

COMPETING INTERESTS

The authors declare no competing interests exist.

MATERIAL AND METHODS

Yeast strains and growth conditions. Yeast strains used in this study are listed in Table 1 and were generated and propagated using standard yeast genetics methods. Yeast strains used in Supplementary Figure 1 were taken from the heterozygote yeast deletion collection

(ThermoFisher) For nicotinamide (NAM) treatments, asynchronously growing cells were centrifuged and resuspended at 0.01-0.1 OD/mL in YPD or synthetic medium containing 20 mM NAM (Sigma-Aldrich). Cells were incubated on a shaker for indicated time. Cells synchronization in G1 was performed by incubating MATa yeasts in medium containing 2 µg/mL alpha-factor for 90 minutes followed by the addition of a second dose of 2 µg/mL of alpha-factor for another 75 minutes. Cells were then washed once in YPD or synthetic medium and released in S phase in medium supplemented with 5 µg/mL pronase (Protease from *Streptomyces griseus*, Sigma-Aldrich). For ionizing irradiation, exponentially growing cells were exposed to 40 Gy followed by a 60-minute incubation at 30°C prior to sample collection. For methyl methane sulfonate (MMS) treatment, cells were first synchronized in G1 using alpha factor, then incubated in YPD containing 0.01% MMS (Sigma -Aldrich) and 5 µg/mL pronase at a density of 1 OD_{630}/mL for 60 minutes. After treatment, cells were washed twice with YPD containing 2.5% sodium thiosulfate (Bioshop), followed by incubation in YPD. Caffeine (Sigma-Aldrich) was used at a concentration of 0.15%.

TABLE 1. Yeast strains used in this study

Strain name	Genotype	Figure	Reference
AE54	BY4743 MATa/α *his3d1/his3d1 leu2d0/leu2d0* LYS2/l*ys2d0 met15d0/MET15 ura3d0/ura3d0*	1D	This study
BW55	BY4743 MATa/α *ura3Δ0 leu2Δ0 his3Δ1 lys2Δ0/LYS+ met15Δ0/MET15+ can1Δ::LEU2+-MFA1pr-HIS3/CAN1+ cdc6Δ::KANMX/CDC6*	1D	Het. Diploid yeast collection
BW57	BY4743 MATa/α *ura3Δ0 leu2Δ0 his3Δ1 lys2Δ0/LYS+ met15Δ0/MET15+ can1Δ::LEU2+-MFA1pr-HIS3/CAN1+ cdc7Δ::KANMX/CDC7*	1D	Het. Diploid yeast collection
BW65	BY4743 MATa/α *ura3Δ0 leu2Δ0 his3Δ1 lys2Δ0/LYS+ met15Δ0/MET15+ can1Δ::LEU2+-MFA1pr-HIS3/CAN1+ dbf4Δ::KANMX/DBF4*	1D	Het. Diploid yeast collection
BW69	BY4743 MATa/α *ura3Δ0 leu2Δ0 his3Δ1 lys2Δ0/LYS+ met15Δ0/MET15+ can1Δ::LEU2+-MFA1pr-HIS3/CAN1+ orc5Δ::KANMX/ORC5*	1D	Het. Diploid yeast collection

BW61	BY4743 MATa/α *ura3Δ0 leu2Δ0 his3Δ1 lys2Δ0/LYS+ met15Δ0/MET15+ can1Δ::LEU2+-MFA1pr-HIS3/CAN1+ rfa1Δ::KANMX/RFA1*	1D	Het. Diploid yeast collection
BW63	BY4743 MATa/α *ura3Δ0 leu2Δ0 his3Δ1 lys2Δ0/LYS+ met15Δ0/MET15+ can1Δ::LEU2+-MFA1pr-HIS3/CAN1+ rfa2Δ::KANMX/RFA2*	1D	Het. Diploid yeast collection
BW59	BY4743 MATa/α *ura3Δ0 leu2Δ0 his3Δ1 lys2Δ0/LYS+ met15Δ0/MET15+ can1Δ::LEU2+-MFA1pr-HIS3/CAN1+ sld3Δ::KANMX/SLD3*	1D	Het. Diploid yeast collection
BX4	BY4743 MATa/α *ura3Δ0 leu2Δ0 his3Δ1 lys2Δ0/LYS+ met15Δ0/MET15+ can1Δ::LEU2+-MFA1pr-HIS3/CAN1+ slx4Δ::KANMX/SLX4*	1D	Het. Diploid yeast collection
BX6	BY4743 MATa/α *ura3Δ0 leu2Δ0 his3Δ1 lys2Δ0/LYS+ met15Δ0/MET15+ can1Δ::LEU2+-MFA1pr-HIS3/CAN1+ pph3Δ::KANMX/PPH3*	1D	Het. Diploid yeast collection
BW79	BY4743 MATa/α *ura3Δ0 leu2Δ0 his3Δ1 lys2Δ0/LYS+ met15Δ0/MET15+ can1Δ::LEU2+-MFA1pr-HIS3/CAN1+ yku70Δ::KANMX/YKU70*	1D	Het. Diploid yeast collection
BW81	BY4743 MATa/α *ura3Δ0 leu2Δ0 his3Δ1 lys2Δ0/LYS+ met15Δ0/MET15+ can1Δ::LEU2+-MFA1pr-HIS3/CAN1+ srs2Δ::KANMX/SRS2*	1D	Het. Diploid yeast collection
BW73	BY4743 MATa/α *ura3Δ0 leu2Δ0 his3Δ1 lys2Δ0/LYS+ met15Δ0/MET15+ can1Δ::LEU2+-MFA1pr-HIS3/CAN1+ taf5Δ::KANMX/TAF5*	1D	Het. Diploid yeast collection
BW75	BY4743 MATa/α *ura3Δ0 leu2Δ0 his3Δ1 lys2Δ0/LYS+ met15Δ0/MET15+ can1Δ::LEU2+-MFA1pr-HIS3/CAN1+ taf12Δ::KANMX/TAF12*	1D	Het. Diploid yeast collection
AV46	W303 MATa *ade2-1 trp1-1 can1-100 leu2-3,112 his3-11,15 ura3d GAL psi+ bar1Δ GAL-MHT*	2A	[11,64]
AV49	W303 MATa *ade2-1 trp1-1 can1-100 leu2-3,112 his3-11,15 ura3d GAL psi+ bar1Δ dbf4-1 GAL-MHT*	2A	[11,64]
BY47	W303 MATα *ade2-1 ura3-1 his3-11,15 leu2-3-112 trp1-1 can1-100*	2A-2C	This study
BY49	W303 MATa *ade2-1 ura3-1 his3-11,15 leu2-3-112 trp1-1 can1-100 cdc7-4*	2A-2C	This study
BY76	W303 MATa *ade2-1 ura3-1 his3-11,15 leu2-3-112 trp1-1 can1-100 bob1-1*	2B	This study

BY77	W303 MATa *ade2-1 ura3-1 his3-11,15 leu2-3-112 trp1-1 can1-100 bob1-1 cdc7Δ::HIS3*	2B	This study
CD28	W303 MATa *ade2-1 ura3-1 his3-11,15 leu2-3-112 trp1-1 can1-100*	2D, 3B-D, 3F-H, 4A, 5A-C	This study
CD30	W303 MATa *ade2-1 ura3-1 his3-11,15 leu2-3-112 trp1-1 can1-100 cdc7-4*	3F-H, 4A, 4C-I, 5A-G, 6A-C, 6F	This study
CD31	W303 MATa *ade2-1 ura3-1 his3-11,15 leu2-3-112 trp1-1 can1-100 rif1d::NATMX*	2D, 3B-D, 3F-G, 4A	This study
CD32	W303 MATa *ade2-1 ura3-1 his3-11,15 leu2-3-112 trp1-1 can1-100 cdc7-4 rif1d::NATMX*	3F-G, 4A	This study
BY51	W303 MATα *ade2-1 ura3-1 his3-11,15 leu2-3-112 trp1-1 can1-100 rif1d::NATMX*	2C	This study
BY53	W303 MATα *ade2-1 ura3-1 his3-11,15 leu2-3-112 trp1-1 can1-100 cdc7-4 rif1d::NATMX*	2C	This study
BX29	W303 MATa *ade2-1 ura3-1 his3-11,15 leu2-3-112 trp1-1 can1-100 cdc7-4 rif1d2-176-13MYC::HIS3MX6*	2C	[35]
BX33	W303 MATa *ade2-1 ura3-1 his3-11,15 leu2-3-112 trp1-1 can1-100 cdc7-4 rif1-RVxF/SILK*	2C	[35]
G26	W303 MATa *ade2-1 ura3-1 his3-11,15 leu2-3-112 trp1-1 can1-100 ADE2 RAD5 RAD52-YFP*	2E	This study
BI43	W303 MATa *ade2-1 ura3-1 his3-11,15 leu2-3-112 trp1-1 can1-100 ADE2 RAD5 RAD52-YFP rif1d::URA3MX*	2E	This study
AZ61	BY4743 MATa/α *ura3Δ0/ura3Δ0 leu2Δ0/leu2Δ0 his3Δ1/his3Δ1 est2d::HPHMXMX/EST2*	2F-G	This study
BL35	BY4743 MATa/α *ura3Δ0/ura3Δ0 leu2Δ0/leu2Δ0 his3Δ1/his3Δ1 est2d::HPHMXMX/EST2 rif1d::URA3MX/RIF1*	2F-G	This study
BB35	BY4743 MATa *ura3Δ0 leu2Δ0 his3Δ1 hst3Δ::HPHMXMX hst4Δ::NATMX [*pCEN-HST3::URA*]*	3A	This study
BJ38	BY4743 MATa *ura3Δ0 leu2Δ0 his3Δ1 hst3Δ::HPHMXMX hst4Δ::NATMX sir2Δ::KANMX rif1Δ::HIS3MX [pCEN-HST3::URA]*	3A	This study
BJ41	BY4743 MATa *ura3Δ0 leu2Δ0 his3Δ1 hst3Δ::HPHMXMX hst4Δ::NATMX sir2Δ::KANMX [pCEN-HST3::URA]*	3A	This study
BJ42	BY4743 MATa *ura3Δ0 leu2Δ0 his3Δ1 hst3Δ::HPHMXMX hst4Δ::NATMX rif1Δ::HIS3MX [pCEN-HST3::URA]*	3A	This study
CF56	W303 MATa *ade2-1 ura3-1 his3-11,15 leu2-3-112 trp1-1 can1-100 rtt109Δ::KANMX6*	3B, 6A, 6C	This study
CD29	W303 MATa *ade2-1 ura3-1 his3-11,15 leu2-3-112 trp1-1 can1-100 hst3Δ::HIS5+ hst4Δ::KANMX*	3B-D, 3F-G, 4A, 5A-C, 6A	This study

CD33	W303 MATa *ade2-1 ura3-1 his3-11,15 leu2-3-112 trp1-1 can1-100 hst3Δ::HIS5+ hst4Δ::KANMX cdc7-4*	3B-D, 3F-H, 4A-I, 5A-G, 6A-F	This study
CC60	BY4741 MATa *ura3Δ0 leu2Δ0 his3Δ1 met15Δ0 Rad52-GFP::HIS3MX*	3E	This study
CC62	BY4741 MATa *ura3Δ0 leu2Δ0 his3Δ1 met15Δ0 Rad52-GFP::HIS3MX rif1Δ::KANMX*	3E	This study
CC64	BY4741 MATa *ura3Δ0 leu2Δ0 his3Δ1 met15Δ0 Rad52-GFP::HIS3MX hst3Δ::HPHMXMX hst4Δ::NATMX*	3E	This study
CC66	BY4741 MATa *ura3Δ0 leu2Δ0 his3Δ1 met15Δ0 Rad52-GFP::HIS3MX hst3Δ::HPHMXMX hst4Δ::NATMX rif1Δ::KANMX*	3E	This study
CD35	W303 MATa *ade2-1 ura3-1 his3-11,15 leu2-3-112 trp1-1 can1-100 hst3Δ::HIS5+ hst4Δ::KANMX cdc7-4 rif1Δ::NATMX*	3F-G, 4A	This study
K11	W303 MATa *ade2-1 ura3-1 his3-11,15 leu2-3-112 trp1-1 can1-100 hst3Δ::HIS5+*	3H	From Alain Verreault's lab
CB63	W303 MATα *ade2-1 ura3-1 his3-11,15 leu2-3-112 trp1-1 can1-100 cdc7-4 hst3Δ::HIS5+*	3H	This study
CH64	W303 MATa *ade2-1 ura3-1 his3-11,15 leu2-3-112 trp1-1 can1-100 hst4Δ::KANMX*	3H	This study
CH67	W303 MATα *ade2-1 ura3-1 his3-11,15 leu2-3-112 trp1-1 can1-100 hst4Δ::KANMX cdc7-4*	3H	This study
K13	W303 MATa *ade2-1 ura3-1 his3-11,15 leu2-3-112 trp1-1 can1-100 hst3Δ::HIS5+ hst4Δ::KANMX*	3F, 6C	[19]
CA15	W303 MATa *ade2-1 ura3-1 his3-11,15 leu2-3-112 trp1-1 can1-100 hst3Δ::HIS5+ hst4Δ::KANMX rif1Δ::NATMX*	3F, 4A	This study
CF50	W303 MATa *ade2-1 ura3-1 his3-11,15 leu2-3-112 trp1-1 can1-100 hst3Δ::HIS5+ hst4Δ::KANMX cdc7-4 [pCEN-HST3-URA3]*	4B	This study
CF48	W303 MATa *ade2-1 ura3-1 his3-11,15 leu2-3-112 trp1-1 can1-100 rad9Δ::HPHMXMX hst3Δ::HIS5+ hst4Δ::KANMX*	5C	This study
CF23	W303 MATa *ade2-1 ura3-1 his3-11,15 leu2-3-112 trp1-1 can1-100 rad9Δ::HPHMX cdc7-4*	5C	This study
CF26	W303 MATa *ade2-1 ura3-1 his3-11,15 leu2-3-112 trp1-1 can1-100 rad9Δ::HPHMX cdc7-4 hst3Δ::HIS5+ hst4Δ::KANMX*	5C	This study
CG29	W303 MATa *ade2-1 ura3-1 his3-11,15 leu2-3-112 trp1-1 can1-100 cdc7-4 mrc1Δ::HIS5+ pRS405-mrc1aq::LEU2*	5D	This study

CG27	W303 MATa *ade2-1 ura3-1 his3-11,15 leu2-3-112 trp1-1 can1-100 hst3Δ::HIS5+ hst4Δ::KANMX mrc1Δ::HIS5+ [pRS405-mrc1aq::LEU2]*	5D	This study
CG23	W303 MATa *ade2-1 ura3-1 his3-11,15 leu2-3-112 trp1-1 can1-100 cdc7-4 hst3Δ::HIS5+ hst4Δ::KANMX mrc1Δ::HIS5+ [pRS405-mrc1aq::LEU2]*	5D	This study
CH44	W303 MATa ade2-1 ura3-1 his3-11,15 leu2-3-112 trp1-1 can1-100 cdc7-4 hst3Δ::HIS5+ hst4Δ::KANMX dbf4Δ::TRP1 his3::PDBF4-dbf4-4A::HIS3 sld3-38A-10his-13MYC::KANMX4	5G	This study
CG53	W303 MATa ade2-1 ura3-1 his3-11,15 leu2-3-112 trp1-1 can1-100 cdc7-4 dbf4Δ::TRP1 his3::PDBF4-dbf4 4A::HIS3 sld3-38A-10his-13MYC::KANMX4	5G	This study
W43	W303 MATα *ade2-1 ura3-52 his3-11,15 leu2-3-112 trp1-1 can1-100*	6A-C	This study
CD78	W303 MATa *ade2-1 ura3-1 his3-11,15 leu2-3-112 trp1-1 can1-100 cdc7-4 rtt109Δ::KANMX*	6A-C	This study
CG14	W303 MATa *ade2-1 ura3-1 his3-11,15 leu2-3-112 trp1-1 can1-100 hst3Δ::HIS5+ hst4Δ::KANMX cdc7-4 rtt109Δ::KANMX*	6A-C	This study
CH73	W303 MATa *ade2-1 ura3-1 his3-11,15 leu2-3-112 trp1-1 can1-100 hht1-hhf1Δ::LEU2 trp1::HHT1-HHF1::TRP1 hst3Δ::HIS5+ hst4Δ::KANMX cdc7-4*	6D-E	This study
CH72	W303 MATα *ade2-1 ura3-1 his3-11,15 leu2-3-112 trp1-1 can1-100 hht1-hhf1Δ::LEU2 trp1::HHT1 K56R-HHF1::TRP1 hst3Δ::HIS5+ hst4Δ::KANMX cdc7-4*	6D-E	This study
B52	W303 MATa *ade2-1 ura3-1 his3-11,15 leu2-3-112 trp1-1 can1-100 hht1-hhf1Δ::LEU2 hht2-hhf2Δ::KANMX3 trp1::HHT1-HHF1::TRP1*	6E	[55]
B51	W303 MATa a*de2-1 ura3-1 his3-11,15 leu2-3-112 trp1-1 can1-100 hht1-hhf1Δ::LEU2 hht2-hhf2Δ::KANMX3 trp1::HHT1 K56R-HHF1::TRP1*	6E	[55]
CH59	W303 MATα *ade2-1 ura3-1 his3-11,15 leu2-3-112 trp1-1 can1-100 rtt101Δ::URA3MX cdc7-4*	6F	This study
CH55	W303 MATα *ade2-1 ura3-1 his3-11,15 leu2-3-112 trp1-1 can1-100 rtt101Δ::URA3MX hst3Δ::HIS5+ hst4Δ::KANMX cdc7-4*	6F	This study
CH68	W303 MATa *ade2-1 ura3-1 his3-11,15 leu2-3-112 trp1-1 can1-100 mms1Δ::URA3MX cdc7-4*	6F	This study
CH71	W303 MATa *ade2-1 ura3-1 his3-11,15 leu2-3-112 trp1-1 can1-100 mms1Δ::URA3MX hst3Δ::HIS5+ hst4Δ::KANMX cdc7-4*	6F	This study

Genome-wide fitness screen. The heterozygote diploid yeast fitness screen was realized as described [65–67]. Briefly, pools of the yeast hetetozygote diploid deletion mutant collection (BY4743 background) were incubated at 30°C in YPD +/- 41 mM NAM. Cells were collected after 20 generations. PCR reactions were performed on extracted DNA to amplify sequence barcodes, and products were used to probe high-density oligonucleotide Affymetrix TAG4 DNA microarrays. Hybridization, washing, staining, scanning and intensity values calculation were performed as described [65–67]. For Z-score calculation, the intensity value of each mutant was divided by the standard deviation. Gene ontology (GO) Term Finder tool was used from the Saccharomyces Genome Database to identify cellular processes affected by NAM treatment [68,69]. Processes identified were considered significant if P-values ≤ 0.01. REViGO was used to summarized significant GO term identified by removing redundant ones [70]. Top 1% genes (Z-score > 2.58 or < -2.58) were compared to a previously published screen (performed on homozygote diploid mutants [26]) using Venn diagrams.

Competitive growth assay

0.0005 OD_{630} of heterozygous deletion and WT diploid yeast cultures were mixed and incubated in YPD +/- 41 mM NAM at 25°C in a 96-well plate. Throughout the incubation, OD_{630} were taken and cells were diluted appropriately to prevent saturation of the culture. After 20 generations, 0.01 OD_{630} of cells was spread on YPD-agar +/- G418 plates. Plates were incubated at 30°C for 48 h and colonies were then counted. The following formula was used to describe growth +/- NAM:

((NAM:G418)/(NAM:YPD))/((YPD:G418)/(YPD:YPD))

NAM:G418 is the number of colonies from cells that were grown in YPD + 41 mM NAM and then plated on YPD + 200 µg/mL G418. NAM:YPD is the number of colonies from cells grown on YPD + 41 mM NAM and then plated on YPD. YPD:G418 is the number of colonies from cells grown on YPD and then plated on YPD + 200 µg/mL G418. YPD:YPD is the number of colonies from cells grown on YPD and then plated on YPD.

Yeast growth assays. For growth in liquid medium, cells were grown to saturation in YPD in a 96-well plate. Cells were then diluted in fresh medium to 0.0005 OD_{630}/ml in 100 µL of YPD containing appropriate concentrations of NAM (Sigma-Aldrich). Cells were then incubated at the indicated temperature for 48-72 h. OD_{630} was then determined using a Biotek EL800 plate reader equipped with Gen5 version 1.05 software. Wells containing YPD were used as blanks. For spot growth assays on solid media, cells were grown in YPD in a 96-well plate to equivalent OD_{630}. Cells were serially diluted 1:5 and spotted on medium containing nicotinamide (Sigma-Aldrich), methyl methane sulfonate (Sigma-Aldrich), hydroxyurea (BioBasics), or 5-Fluoroorotic acid (Bioshop). Plates were incubated at the indicated temperature for 48-72 h.

Cell cycle analysis by flow cytometry. DNA content/cell cycle analysis by flow cytometry was performed as described previously [71]. Flow cytrometry was performed using a BD Biosciences FACSCalibur instrument equipped with CellQuest software. Data were analyzed using FlowJo 10.8.1 (FlowJo, LLC).

Immunoblotting. 4 OD of cells were pelleted and frozen at -80°C prior whole-cell extraction. Cells were extracted using 0.1M NaOH for 5 minutes at room temperature as described before [72] or using standard tri-chloroacetic acid (TCA) and glass beads method [73]. Protein extracts were quantified using bicinchoninic acid (BCA) protein assay kit according to the manufacturer's protocol (Pierce). SDS-PAGE and transfer were performed using standard methods. Anti-H3 (ab1791) and anti-Rad53 (ab104232) were purchased from abcam. Anti-H3K56ac (AV105) and anti-H2A-S129-P (AV137) antibodies were generously provided by Dr. Alain Verreault (Université de Montréal, Canada). Goat anti-rabbit (BioRad; cat: 1705046), goat anti-mouse (Bio Rad; cat: 1705047) and goat anti-rat (Abcam; cat: ab97057) were used as secondary antibodies. Protein visualization was realized by chemiluminescence using Pierce ECL Western Blotting Substrate. Images were captured using an Azure c600 chemiluminescence Imaging System.

Fluorescence microscopy. Cells were fixed in 0.1M of potassium phosphate buffer pH 6.4 containing 3.7% formaldehyde (Sigma-Aldrich) and slides were prepared as described [48].

Images were taken by fluorescence microscopy using a 60X objective (numerical aperture [NA], 1.42) on DeltaVision instrument (GE Healthcare). Images analysis was performed using SoftWoRx 7 software and FIJI 1.53.

Measurement of DNA content by quantitative PCR. Genomic DNA from 1 OD_{630} of cells was extracted and purified as described [74]. 3 ng of DNA was used per qPCR reaction (qPCR Master Mix, NEB). PCR was performed using an Applied Biosystems 7500 instrument (software version 2.3). PCR primers are listed in Table 1. Briefly, qPCR signal for a given origin was first normalized to the signal obtained from the NegV locus (ChrV: 532538-532516) [62]. This region is located ≈12 Kb from ARS521, an origin which has not been detected to be active in several studies according to OriDB (http://cerevisiae.oridb.org/) and ≈18 kb from ARS522, a subtelomeric origin of replication activated in late S. As such, the NegV locus is expected to be replicated in very late S, and therefore to generally remain unreplicated in a majority of *cdc7-4* and *cdc7-4 hst3*Δ *hst4*Δ cells 30 minutes post-release from G1 arrest toward S phase. The NegV-normalized S phase signal was divided by the NegV-normalized signal obtained from alpha factor arrested (G1) cells. Complete replication of an origin is therefore expected to result in a ratio of S phase over G1 signal of 2.

TABLE 2: PCR primers used in this study.

Primer Name	**Sequence (5'-3')**
ARS305_qPCR_F	TACACGGGGGCTAAAAACGG
ARS305_qPCR_R	GCACTTTGATGAGGTCTCTAGC
ARS607_qPCR_F	GGCTCGTGCATTAAGCTTGT
ARS607_qPCR_R	CACGCCAAACATTGCATTTA
ARS1211_qPCR_F	TTGGGCTAGGAGAAAGTGGC
ARS1211_qPCR_R	CGAACGCAATGTGCCAAGAA
ARS315_qPCR_F	TTCTTCGCGCGTCAACTTTC
ARS315_qPCR_R	TTTCTTGGCGCTACGATGTG
ARS300-F	TCACCCATCTCTCACCATCA

ARS300-R	GATGGGCGTTATGCGTAAAT
NegV_qPCR_F	TAATTGCTGAGCGTTGCATGTT
NegV_qPCR_R	GCCTCTACAGTACCGTGGGGAGA
ARS305_probe_F	ATCGTGTAAGCTGGGGTGAC
ARS305_probe_R	AGTGGCGTTAGGTTCAATGC

Alkaline gel electrophoresis and Southern blotting. Samples were denatured by heating at 70°C in loading buffer (30 mM NaOH, 1 mM EDTA, 3% Ficoll 400, 0.01% bromocresol green). Denatured DNA was run in a 1% agarose gel in alkaline electrophoresis buffer (30 mM NaOH, 2 mM EDTA) at 3 V/cm. Southern blotting was performed using a digoxygenin (DIG)-labeled probe as described [75]. The ARS305 probe was generated by PCR using primers ARS305_probe_F and ARS305_probe_R (Table 1) and the PCR DIG Labeling Mix (Roche). Membranes were imaged using an Azure c600 chemiluminescence Imaging System.

Statistical analysis. Data are represented as mean ± standard error of the mean (SEM) unless otherwise specified. All analyses were performed using GraphPad Prism 8. Statistical tests used are described in figure legends.

FIGURE LEGENDS

FIGURE 1. A screen to identify haploinsufficent genes modulating cell fitness upon NAM exposure. (A) Z-score of individual heterozygote diploid yeast strains after 20 generations in medium containing 41mM NAM. GO-terms of genes for which the Z-scores is > 2.58 or < -2.58 were further analyzed in C. (B) Venn diagram comparing the heterozygote diploid screen presented in this article with a previously published screen using homozygote diploid deletion strains [26]. (C) GO-term associated with genes presenting Z-scores > 2.58 or < -2.58. (D) Growth competition assay for selected heterozygote mutant strains in 1:1 competition with a WT. WT and

mutant cells were mixed 1:1 and grown in YPD +/- 41 mM NAM for 20 generations. The fraction of mutant/WT cells in the culture was assessed by plating on selective medium followed by colony counting. Colors and numbers below strain names refer to GO-terms listed in C.

FIGURE 2. Compromised DDK-dependent activation of origins of DNA replication sensitizes cells to NAM. (A) Haploid *dbf4-1* and *cdc7-4* cells are sensitive to NAM at their semi-permissive temperature. Cells were incubated at 30°C in medium containing the indicated concentration of NAM. OD_{630} readings were taken at 72 h to evaluate cell proliferation (see Methods). (B) *bob1-1 cdc7*Δ cells are not sensitive to NAM. 5-fold serial dilutions of cells were spotted on YPD-agar and incubated at the indicated temperature. (C) The Glc7-interacting motif of Rif1 causes NAM sensitivity in *cdc7-4* cells. Cells were treated as in B. (D) NAM-induced phosphorylation of H2A-S129 is reduced upon deletion of *RIF1*. WT and *rif1Δ* cells were exposed to 20 mM NAM for 8 h at 30°C before harvest for immunoblotting. (E) Deletion of *RIF1* reduces the frequency of Rad52-YFP foci in response to NAM, but not upon IR treatment. Exponential growing cells were treated in medium containing 20 mM NAM for 8h at 30°C, or exposed to 40 Grey of ionizing radiations followed by incubation for 1 h at 30°C. Samples were then taken for fluorescence microscopy. Graph bars represent mean ± SEM of three independent experiments. (F) *rif1*Δ rescues the NAM sensitivity of *est2Δ* strains. OD_{630} readings of treated vs untreated cells after 48h of growth in 96-wells plates is presented. Graph bars represent mean ± SEM of three independent experiments each containing 4 technical replicates. **: p value < 0.01 and ***: p value < 0.001, Student's *t*-test. (G) *RIF1* deletion reduces NAM-induced S phase accumulation. Exponentially growing cells were incubated at 25°C in YPD containing 20 mM NAM for 8 h. Samples were taken for flow cytometry analysis of DNA content.

FIGURE 3. The activity of replication origins influences the phenotypes of *hst3Δ hst4Δ* cells. (A) Deletion of *RIF1* rescues the temperature sensitivity of *hst3Δ hst4Δ* cells (in the BY4741 genetic background) as well as the synthetic lethality of *hst3Δ hst4Δ sir2Δ* triple mutant. 5-fold serial dilutions of cells were spotted on the indicated medium and incubated at the indicated temperature. (B) Rif1 does not modulate H3 K56ac levels. Exponentially growing cells in YPD at 25°C were harvested and processed for immunoblotting. (C) *RIF1* deletion improves S phase progression of *hst3Δ hst4Δ* cells after transient exposure to MMS. Exponentially growing cells at 25°C in YPD were arrested in G1 using alpha factor and released toward S in medium containing 0.01% of MMS for 90 minutes (MMS time point). After MMS inactivation using sodium thiosulfate, cells were released in fresh YPD. Samples were taken for flow cytometry analysis of DNA content at the indicated time points. As: asynchronous. (D) Deletion of *RIF1* does not rescue the sensitivity of *hst3*Δ *hst4*Δ cells to MMS. 5-fold serial dilutions of cells were spotted on the indicated media and incubated at the indicated temperature. (E) *RIF1* elevates the frequency of spontaneous Rad52 foci formation in *hst3Δ hst4Δ* cells. Rad52-GFP foci was assessed by fluorescence microscopy in exponentially growing cells at 25°C. Graph bars represent mean value ± SEM of 10 independent experiments. **: p value < 0.01 Student's *t*-test. (F) Deletion of *RIF1* reduces intra-S phase checkpoint activation in *cdc7-4 hst3Δ hst4Δ* strain. Exponentially growing cells in YPD at 25°C were harvested for immunoblotting. MMS: Cells were exposed to 0.03% MMS for 1 h prior to harvesting as control. (G) *hst3Δ hst4Δ cdc7-4* cells present strong synthetic temperature sensitivity. 5-fold serial dilutions of cells were spotted on YPD-agar and incubated at the indicated temperature. (H) Individual deletion of *HST3* or *HST4* gene in *cdc7-4* does not cause

synthetic temperature sensitivity. 5-fold serial dilutions of cells were spotted on YPD-agar and incubated at the indicated temperature.

FIGURE 4. Deletion of *HST3* and *HST4* inhibits the activation of origins of replication in *cdc7-4* cells. (A) S phase progression is impaired in *cdc7-4 hst3Δ hst4Δ* cells at the semi-permissive temperature for cdc7-4. Exponentially growing cells were arrested in G1 at 25°C and released toward S phase at 30°C. Samples were taken for DNA content analysis by flow cytometry at the indicated time points. As: Asynchronous exponentially growing cells. (B) Expression of Hst3 restores S phase progression of *cdc7-4 hst3Δ hst4Δ* cells at 30°C. Cells were treated as in A. (C) Incubation of asynchronous *cdc7-4 hst3Δ hst4Δ* cells at 30°C causes them to accumulate in early S phase. Asynchronously growing cells were transferred from 25°C to 30°C for the indicated time and harvested for DNA content determination by flow cytometry. (D-E) *cdc7-4 hst3Δ hst4Δ* cells accumulating with DNA content near 1N at 30°C are budded. (D) Cells were treated as in A and processed for DNA content analysis by flow cytometry. (E) Budding index of cells harvested in D. 200 cells were manually inspected per condition. (F) Activation of early origin of DNA replication is compromised in *cdc7-4 hst3Δ hst4Δ* cells released from G1 toward S phase at the semi-permissive temperature for *cdc7-4* (30°C). Cells were treated as in A and harvested 30 minutes post-release toward S phase at 30°C. DNA was extracted and processed for quantitative PCR analysis as described in Material and Methods. qPCR signal for a given origin was normalized to that obtained from the NegV locus (which is expected to be unreplicated in most cells 30 minutes post-release from G1 toward S). Normalized signals were then divided by the normalized signals obtained from alpha factor arrested (G1) cells. Graph bars represent mean ± SEM of five independent experiments. *: p value < 0.05 and **: p value < 0.01, Student's t-test. (G) *cdc7-4*

hst3Δ hst4Δ eventually complete S phase with delayed kinetics. Cells were treated as in A. (H) Origin DNA is duplicated with delayed kinetics in *cdc7-4 hst3Δ hst4Δ* cells. As in F, except that cells were released toward S phase in presence of 200 mM HU for 120 minutes at 30°C prior harvest. Graph bars represent mean ± SEM of three independent experiments. (I) Formation of nascent DNA is inhibited at the early origin ARS305 origin in *cdc7-4 hst3Δ hst4Δ* cells. Cells were treated as in A. DNA samples were run on alkaline gels followed by Southern blotting to detect short ssDNA fragments generated at ARS305 upon origin activation.

FIGURE 5. S phase progression defects of *cdc7-4 hst3Δ hst4Δ* is not due to the activation of the checkpoint. (A-B) Rad53 activation is inhibited *cdc7-4 hst3Δ hst4Δ* upon release from G1 arrest toward S phase in the presence of HU. Cells were arrested in G1 using alpha factor at 25°C and released toward S phase at 30°C in presence or absence of 200 mM HU. (A) Cells were harvested for 60 minutes post-release toward S and processed for immunoblotting. (B) Samples were also taken for DNA content analysis by flow cytometry. As: Asynchronously growing cells. (C) *RAD9* deletion modestly improves S phase progression of *cdc7-4 hst3Δ hst4Δ* cells, but only at later time points. Exponentially growing cells were arrested in G1 using alpha factor at 25°C and released toward S at 30°C. Samples were taken for DNA content analysis by flow cytometry at the indicated time points. (D) Mutation of *MRC1* that inhibit its functions in the intra S phase checkpoint response (*mrc1*-AQ) does not improve S phase progression of *cdc7-4 hst3Δ hst4Δ* cells at 30°C. Cells were treated and collected as in C. (E-F) Caffeine does not improve S phase progression of *cdc7-4 hst3Δ hst4Δ* at 30°C. Exponentially growing cells were arrested in G1 using alpha factor at 25°C and released toward S phase at 30°C in YPD +/- 200 mM HU and +/- 0.15% caffeine. (E) After 60 minutes in S, cells were harvested for immunoblotting. (F) Samples were

taken for DNA content analysis by flow cytometry at the indicated time points. (G) The *dbf4-4A sld3-38A* mutations do not improve S phase progression of *cdc7-4 hst3Δ hst4Δ* cells at 30°C. Cells were treated as in C.

FIGURE 6. Constitutive H3K56 acetylation, Rtt101, and Mms1 cause S phase progression defects and synthetic temperature sensitivity in *cdc7-4 hst3Δ hst4Δ* cells. (A-B) Deletion of *RTT109* rescues S phase progression in *cdc7-4 hst3Δ hst4Δ* cells at the semi-permissive temperature for *cdc7-4* of 29°C. Exponentially growing cells were arrested in G1 at 25°C and released toward S for 60 minutes at 29°C. Samples were taken for DNA content analysis by flow cytometry. (B) Violin plot representation the Sytox Green value (DNA content) per cell from the 60 minutes time point in A. Red bars represent the median and quartiles. ****: p value < 0.0001 Mann-Whitney test. (C) *RTT109* deletion rescue the synthetic temperature sensitivity of *cdc7-4 hst3Δ hst4Δ* cells. 5-fold serial dilutions of cells were spotted on YPD-agar and incubated at the indicated temperature. (D-E) Reducing H3 K56ac levels rescues mutant the synthetic temperature sensitivity of *cdc7-4 hst3Δ hst4Δ* cells. *cdc7-4 hst3Δ hst4Δ HHT2* strains expressing either HHT1 or HHT1-K56R were generated. (D) 5-fold serial dilutions of cells were spotted on YPD-agar and incubated at the indicated temperature. (E) Exponentially growing cells at 25°C were processed for immunoblotting. (F) *RTT101* or *MMS1* deletion rescue the synthetic temperature sensitivity of *cdc7-4 hst3Δ hst4Δ* cells. Cells were treated as in C.

REFERENCES

1. Remus D, Diffley JF. Eukaryotic DNA replication control: Lock and load, then fire. Current Opinion in Cell Biology. 2009;21: 771–777. doi:10.1016/j.ceb.2009.08.002

2. Tanaka T, Umemori T, Endo S, Muramatsu S, Kanemaki M, Kamimura Y, et al. Sld7, an Sld3-associated protein required for efficient chromosomal DNA replication in budding yeast. EMBO J. 2011;30: 2019–2030. doi:10.1038/emboj.2011.115

3. Mantiero D, Mackenzie A, Donaldson A, Zegerman P. Limiting replication initiation factors execute the temporal programme of origin firing in budding yeast. EMBO J. 2011;30: 4805–4814. doi:10.1038/emboj.2011.404

4. Branzei D, Foiani M. The checkpoint response to replication stress. DNA Repair. 2009;8: 1038–1046. doi:16/j.dnarep.2009.04.014

5. Bacal J, Moriel-Carretero M, Pardo B, Barthe A, Sharma S, Chabes A, et al. Mrc1 and Rad9 cooperate to regulate initiation and elongation of DNA replication in response to DNA damage. EMBO J. 2018;37. doi:10.15252/embj.201899319

6. Santocanale C, Diffley JF. A Mec1- and Rad53-dependent checkpoint controls late-firing origins of DNA replication. Nature. 1998;395: 615–618. doi:10.1038/27001

7. Zegerman P, Diffley JFX. Checkpoint-dependent inhibition of DNA replication initiation by Sld3 and Dbf4 phosphorylation. Nature. 2010;467: 474–478. doi:10.1038/nature09373

8. Toledo LI, Altmeyer M, Rask M-B, Lukas C, Larsen DH, Povlsen LK, et al. ATR prohibits replication catastrophe by preventing global exhaustion of RPA. Cell. 2013;155: 1088–1103. doi:10.1016/j.cell.2013.10.043

9. Smith OK, Aladjem MI. Chromatin Structure and Replication Origins: Determinants Of Chromosome Replication And Nuclear Organization. J Mol Biol. 2014;426: 3330–3341. doi:10.1016/j.jmb.2014.05.027

10. Méchali M, Yoshida K, Coulombe P, Pasero P. Genetic and epigenetic determinants of DNA replication origins, position and activation. Curr Opin Genet Dev. 2013;23: 124–131. doi:10.1016/j.gde.2013.02.010

11. Yoshida K, Bacal J, Desmarais D, Padioleau I, Tsaponina O, Chabes A, et al. The histone deacetylases sir2 and rpd3 act on ribosomal DNA to control the replication program in budding yeast. Mol Cell. 2014;54: 691–697. doi:10.1016/j.molcel.2014.04.032

12. Brachmann CB, Sherman JM, Devine SE, Cameron EE, Pillus L, Boeke JD. The SIR2 gene family, conserved from bacteria to humans, functions in silencing, cell cycle progression, and chromosome stability. Genes Dev. 1995;9: 2888–2902.

13. Pasero P, Bensimon A, Schwob E. Single-molecule analysis reveals clustering and epigenetic regulation of replication origins at the yeast rDNA locus. Genes Dev. 2002;16: 2479–2484. doi:10.1101/gad.232902

14. Stevenson JB, Gottschling DE. Telomeric chromatin modulates replication timing near chromosome ends. Genes Dev. 1999;13: 146–151.

15. Irlbacher H, Franke J, Manke T, Vingron M, Ehrenhofer-Murray AE. Control of replication initiation and heterochromatin formation in Saccharomyces cerevisiae by a regulator of meiotic gene expression. Genes Dev. 2005;19: 1811–1822. doi:10.1101/gad.334805

16. Weber JM, Irlbacher H, Ehrenhofer-Murray AE. Control of replication initiation by the Sum1/Rfm1/Hst1 histone deacetylase. BMC Molecular Biology. 2008;9: 100. doi:10.1186/1471-2199-9-100

17. Cockell MM, Perrod S, Gasser SM. Analysis of Sir2p Domains Required for rDNA and Telomeric Silencing in Saccharomyces cerevisiae. Genetics. 2000;154: 1069–1083.

18. Lamming DW, Latorre-Esteves M, Medvedik O, Wong SN, Tsang FA, Wang C, et al. HST2 mediates SIR2-independent life-span extension by calorie restriction. Science. 2005;309: 1861–1864. doi:10.1126/science.1113611

19. Celic I, Masumoto H, Griffith WP, Meluh P, Cotter RJ, Boeke JD, et al. The sirtuins hst3 and Hst4p preserve genome integrity by controlling histone h3 lysine 56 deacetylation. Curr Biol. 2006;16: 1280–1289. doi:10.1016/j.cub.2006.06.023

20. Driscoll R, Hudson A, Jackson SP. Yeast Rtt109 promotes genome stability by acetylating histone H3 on lysine 56. Science. 2007;315: 649–652. doi:10.1126/science.1135862

21. Fillingham J, Recht J, Silva AC, Suter B, Emili A, Stagljar I, et al. Chaperone control of the activity and specificity of the histone H3 acetyltransferase Rtt109. Mol Cell Biol. 2008;28: 4342–4353. doi:10.1128/MCB.00182-08

22. Maas NL, Miller KM, DeFazio LG, Toczyski DP. Cell cycle and checkpoint regulation of histone H3 K56 acetylation by Hst3 and Hst4. Mol Cell. 2006;23: 109–119. doi:10.1016/j.molcel.2006.06.006

23. Celic I, Verreault A, Boeke JD. Histone H3 K56 hyperacetylation perturbs replisomes and causes DNA damage. Genetics. 2008;179: 1769–1784. doi:10.1534/genetics.108.088914

24. Simoneau A, Delgoshaie N, Celic I, Dai J, Abshiru N, Costantino S, et al. Interplay Between Histone H3 Lysine 56 Deacetylation and Chromatin Modifiers in Response to DNA Damage. Genetics. 2015. doi:10.1534/genetics.115.175919

25. Sauve AA, Wolberger C, Schramm VL, Boeke JD. The Biochemistry of Sirtuins. Annual Review of Biochemistry. 2006;75: 435–465. doi:10.1146/annurev.biochem.74.082803.133500

26. Simoneau A, Ricard É, Weber S, Hammond-Martel I, Wong LH, Sellam A, et al. Chromosome-wide histone deacetylation by sirtuins prevents hyperactivation of DNA damage-induced signaling upon replicative stress. Nucleic Acids Res. 2016. doi:10.1093/nar/gkv1537

27. Simoneau A, Ricard É, Wurtele H. An interplay between multiple sirtuins promotes completion of DNA replication in cells with short telomeres. PLoS Genet. 2018;14: e1007356. doi:10.1371/journal.pgen.1007356

28. Irene C, Theis JF, Gresham D, Soteropoulos P, Newlon CS. Hst3p, a histone deacetylase, promotes maintenance of Saccharomyces cerevisiae chromosome III lacking efficient replication origins. Mol Genet Genomics. 2016;291: 271–283. doi:10.1007/s00438-015-1105-8

29. Barazandeh M, Kriti D, Nislow C, Giaever G. The cellular response to drug perturbation is limited: comparison of large-scale chemogenomic fitness signatures. BMC Genomics. 2022;23: 197. doi:10.1186/s12864-022-08395-x

30. Hardy CF, Dryga O, Seematter S, Pahl PM, Sclafani RA. mcm5/cdc46-bob1 bypasses the requirement for the S phase activator Cdc7p. Proc Natl Acad Sci USA. 1997;94: 3151–3155.

31. Davé A, Cooley C, Garg M, Bianchi A. Protein Phosphatase 1 Recruitment by Rif1 Regulates DNA Replication Origin Firing by Counteracting DDK Activity. Cell Reports. 2014;7: 53–61. doi:10.1016/j.celrep.2014.02.019

32. Hayano M, Kanoh Y, Matsumoto S, Renard-Guillet C, Shirahige K, Masai H. Rif1 is a global regulator of timing of replication origin firing in fission yeast. Genes Dev. 2012;26: 137–150. doi:10.1101/gad.178491.111

33. Mattarocci S, Shyian M, Lemmens L, Damay P, Altintas DM, Shi T, et al. Rif1 controls DNA replication timing in yeast through the PP1 phosphatase Glc7. Cell Rep. 2014;7: 62–69. doi:10.1016/j.celrep.2014.03.010

34. Hiraga S-I, Alvino GM, Chang F, Lian H-Y, Sridhar A, Kubota T, et al. Rif1 controls DNA replication by directing Protein Phosphatase 1 to reverse Cdc7-mediated phosphorylation of the MCM complex. Genes Dev. 2014;28: 372–383. doi:10.1101/gad.231258.113

35. Hafner L, Lezaja A, Zhang X, Lemmens L, Shyian M, Albert B, et al. Rif1 Binding and Control of Chromosome-Internal DNA Replication Origins Is Limited by Telomere Sequestration. Cell Rep. 2018;23: 983–992. doi:10.1016/j.celrep.2018.03.113

36. Stead BE, Brandl CJ, Davey MJ. Phosphorylation of Mcm2 modulates Mcm2–7 activity and affects the cell's response to DNA damage. Nucleic Acids Res. 2011;39: 6998–7008. doi:10.1093/nar/gkr371

37. Stead BE, Brandl CJ, Sandre MK, Davey MJ. Mcm2 phosphorylation and the response to replicative stress. BMC Genet. 2012;13: 36. doi:10.1186/1471-2156-13-36

38. Downs JA, Lowndes NF, Jackson SP. A role for Saccharomyces cerevisiae histone H2A in DNA repair. Nature. 2000;408: 1001–1004. doi:10.1038/35050000

39. Lisby M, Rothstein R, Mortensen UH. Rad52 forms DNA repair and recombination centers during S phase. Proc Natl Acad Sci U S A. 2001;98: 8276–8282. doi:10.1073/pnas.121006298

40. Marcand S, Gilson E, Shore D. A Protein-Counting Mechanism for Telomere Length Regulation in Yeast. Science. 1997 [cited 7 Jan 2022]. doi:10.1126/science.275.5302.986

41. Hiraga S-I, Monerawela C, Katou Y, Shaw S, Clark KR, Shirahige K, et al. Budding yeast Rif1 binds to replication origins and protects DNA at blocked replication forks. EMBO Rep. 2018;19. doi:10.15252/embr.201846222

42. Yekezare M, Gómez-González B, Diffley JFX. Controlling DNA replication origins in response to DNA damage – inhibit globally, activate locally. J Cell Sci. 2013;126: 1297–1306. doi:10.1242/jcs.096701

43. Osborn AJ, Elledge SJ. Mrc1 is a replication fork component whose phosphorylation in response to DNA replication stress activates Rad53. Genes Dev. 2003;17: 1755–1767. doi:10.1101/gad.1098303

44. Hall-Jackson CA, Cross DA, Morrice N, Smythe C. ATR is a caffeine-sensitive, DNA-activated protein kinase with a substrate specificity distinct from DNA-PK. Oncogene. 1999;18: 6707–6713. doi:10.1038/sj.onc.1203077

45. Osman F, McCready S. Differential effects of caffeine on DNA damage and replication cell cycle checkpoints in the fission yeast Schizosaccharomyces pombe. Mol Gen Genet. 1998;260: 319–334. doi:10.1007/s004380050901

46. Han J, Zhou H, Horazdovsky B, Zhang K, Xu R-M, Zhang Z. Rtt109 Acetylates Histone H3 Lysine 56 and Functions in DNA Replication. Science. 2007;315: 653–655. doi:10.1126/science.1133234

47. Collins SR, Miller KM, Maas NL, Roguev A, Fillingham J, Chu CS, et al. Functional dissection of protein complexes involved in yeast chromosome biology using a genetic interaction map. Nature. 2007;446: 806–810. doi:10.1038/nature05649

48. Wurtele H, Kaiser GS, Bacal J, St-Hilaire E, Lee E-H, Tsao S, et al. Histone h3 lysine 56 acetylation and the response to DNA replication fork damage. Mol Cell Biol. 2012;32: 154–172. doi:10.1128/MCB.05415-11

49. Han J, Zhang H, Zhang H, Wang Z, Zhou H, Zhang Z. A Cul4 E3 Ubiquitin Ligase Regulates Histone Hand-Off during Nucleosome Assembly. Cell. 2013;155: 817–829. doi:10.1016/j.cell.2013.10.014

50. Roberts TM, Zaidi IW, Vaisica JA, Peter M, Brown GW. Regulation of Rtt107 Recruitment to Stalled DNA Replication Forks by the Cullin Rtt101 and the Rtt109 Acetyltransferase. Mol Biol Cell. 2008;19: 171–180. doi:10.1091/mbc.E07-09-0961

51. Li Q, Zhou H, Wurtele H, Davies B, Horazdovsky B, Verreault A, et al. Acetylation of Histone H3 Lysine 56 Regulates Replication-Coupled Nucleosome Assembly. Cell. 2008;134: 244–255. doi:10.1016/j.cell.2008.06.018

52. Burgess RJ, Zhou H, Han J, Zhang Z. A Role for Gcn5 in Replication-Coupled Nucleosome Assembly. Molecular Cell. 2010;37: 469–480. doi:10.1016/j.molcel.2010.01.020

53. Hammond-Martel I, Verreault A, Wurtele H. Chromatin dynamics and DNA replication roadblocks. DNA Repair (Amst). 2021;104: 103140. doi:10.1016/j.dnarep.2021.103140

54. Thaminy S, Newcomb B, Kim J, Gatbonton T, Foss E, Simon J, et al. Hst3 is regulated by Mec1-dependent proteolysis and controls the S phase checkpoint and sister chromatid cohesion by deacetylating histone H3 at lysine 56. J Biol Chem. 2007;282: 37805–37814. doi:10.1074/jbc.M706384200

55. Masumoto H, Hawke D, Kobayashi R, Verreault A. A role for cell-cycle-regulated histone H3 lysine 56 acetylation in the DNA damage response. Nature. 2005;436: 294–298. doi:10.1038/nature03714

56. Theis JF, Irene C, Dershowitz A, Brost RL, Tobin ML, di Sanzo FM, et al. The DNA Damage Response Pathway Contributes to the Stability of Chromosome III Derivatives Lacking Efficient Replicators. PLoS Genet. 2010;6. doi:10.1371/journal.pgen.1001227

57. Unnikrishnan A, Gafken PR, Tsukiyama T. Dynamic changes in histone acetylation regulate origins of DNA replication. Nat Struct Mol Biol. 2010;17: 430–437. doi:10.1038/nsmb.1780

58. Hoggard T, Müller CA, Nieduszynski CA, Weinreich M, Fox CA. Sir2 mitigates an intrinsic imbalance in origin licensing efficiency between early- and late-replicating euchromatin. Proc Natl Acad Sci USA. 2020;117: 14314–14321. doi:10.1073/pnas.2004664117

59. Vogelauer M, Rubbi L, Lucas I, Brewer BJ, Grunstein M. Histone acetylation regulates the time of replication origin firing. Mol Cell. 2002;10: 1223–1233. doi:10.1016/s1097-2765(02)00702-5

60. Labib K, De Piccoli G. Surviving chromosome replication: the many roles of the S-phase checkpoint pathway. Philos Trans R Soc Lond, B, Biol Sci. 2011;366: 3554–3561. doi:10.1098/rstb.2011.0071

61. Davidson MB, Katou Y, Keszthelyi A, Sing TL, Xia T, Ou J, et al. Endogenous DNA replication stress results in expansion of dNTP pools and a mutator phenotype. EMBO J. 2012;31: 895–907. doi:10.1038/emboj.2011.485

62. Gershon L, Kupiec M. A novel role for Dun1 in the regulation of origin firing upon hyper-acetylation of H3K56. PLoS Genet. 2021;17: e1009391. doi:10.1371/journal.pgen.1009391

63. Mimura S, Yamaguchi T, Ishii S, Noro E, Katsura T, Obuse C, et al. Cul8/Rtt101 Forms a Variety of Protein Complexes That Regulate DNA Damage Response and Transcriptional Silencing. J Biol Chem. 2010;285: 9858–9867. doi:10.1074/jbc.M109.082107

64. Tanaka S, Nakato R, Katou Y, Shirahige K, Araki H. Origin Association of Sld3, Sld7, and Cdc45 Proteins Is a Key Step for Determination of Origin-Firing Timing. Current Biology. 2011;21: 2055–2063. doi:10.1016/j.cub.2011.11.038

65. Ericson E, Hoon S, St Onge RP, Giaever G, Nislow C. Exploring gene function and drug action using chemogenomic dosage assays. Methods Enzymol. 2010;470: 233–255. doi:10.1016/S0076-6879(10)70010-0

66. Smith AM, Durbic T, Oh J, Urbanus M, Proctor M, Heisler LE, et al. Competitive genomic screens of barcoded yeast libraries. J Vis Exp. 2011. doi:10.3791/2864

67. Pierce SE, Davis RW, Nislow C, Giaever G. Genome-wide analysis of barcoded Saccharomyces cerevisiae gene-deletion mutants in pooled cultures. Nat Protoc. 2007;2: 2958–2974. doi:10.1038/nprot.2007.427

68. Boyle EI, Weng S, Gollub J, Jin H, Botstein D, Cherry JM, et al. GO::TermFinder--open source software for accessing Gene Ontology information and finding significantly enriched Gene Ontology terms associated with a list of genes. Bioinformatics. 2004;20: 3710–3715. doi:10.1093/bioinformatics/bth456

69. Cherry JM, Hong EL, Amundsen C, Balakrishnan R, Binkley G, Chan ET, et al. Saccharomyces Genome Database: the genomics resource of budding yeast. Nucleic Acids Res. 2012;40: D700-705. doi:10.1093/nar/gkr1029

70. Supek F, Bošnjak M, Škunca N, Šmuc T. REVIGO Summarizes and Visualizes Long Lists of Gene Ontology Terms. PLoS ONE. 2011;6: e21800. doi:10.1371/journal.pone.0021800

71. Haase SB, Reed SI. Improved flow cytometric analysis of the budding yeast cell cycle. Cell Cycle. 2002;1: 132–136.

72. Kushnirov VV. Rapid and reliable protein extraction from yeast. Yeast. 2000;16: 857–860. doi:10.1002/1097-0061(20000630)16:9<857::AID-YEA561>3.0.CO;2-B

73. Grallert A, Hagan IM. Preparation of Protein Extracts from Schizosaccharomyces pombe Using Trichloroacetic Acid Precipitation. Cold Spring Harb Protoc. 2017;2017: pdb.prot091579. doi:10.1101/pdb.prot091579

74. Dymond JS. Preparation of genomic DNA from Saccharomyces cerevisiae. Methods Enzymol. 2013;529: 153–160. doi:10.1016/B978-0-12-418687-3.00012-4

75. Viterbo D, Marchal A, Mosbach V, Poggi L, Vaysse-Zinkhöfer W, Richard G-F. A fast, sensitive and cost-effective method for nucleic acid detection using non-radioactive probes. Biol Methods Protoc. 2018;3. doi:10.1093/biomethods/bpy006

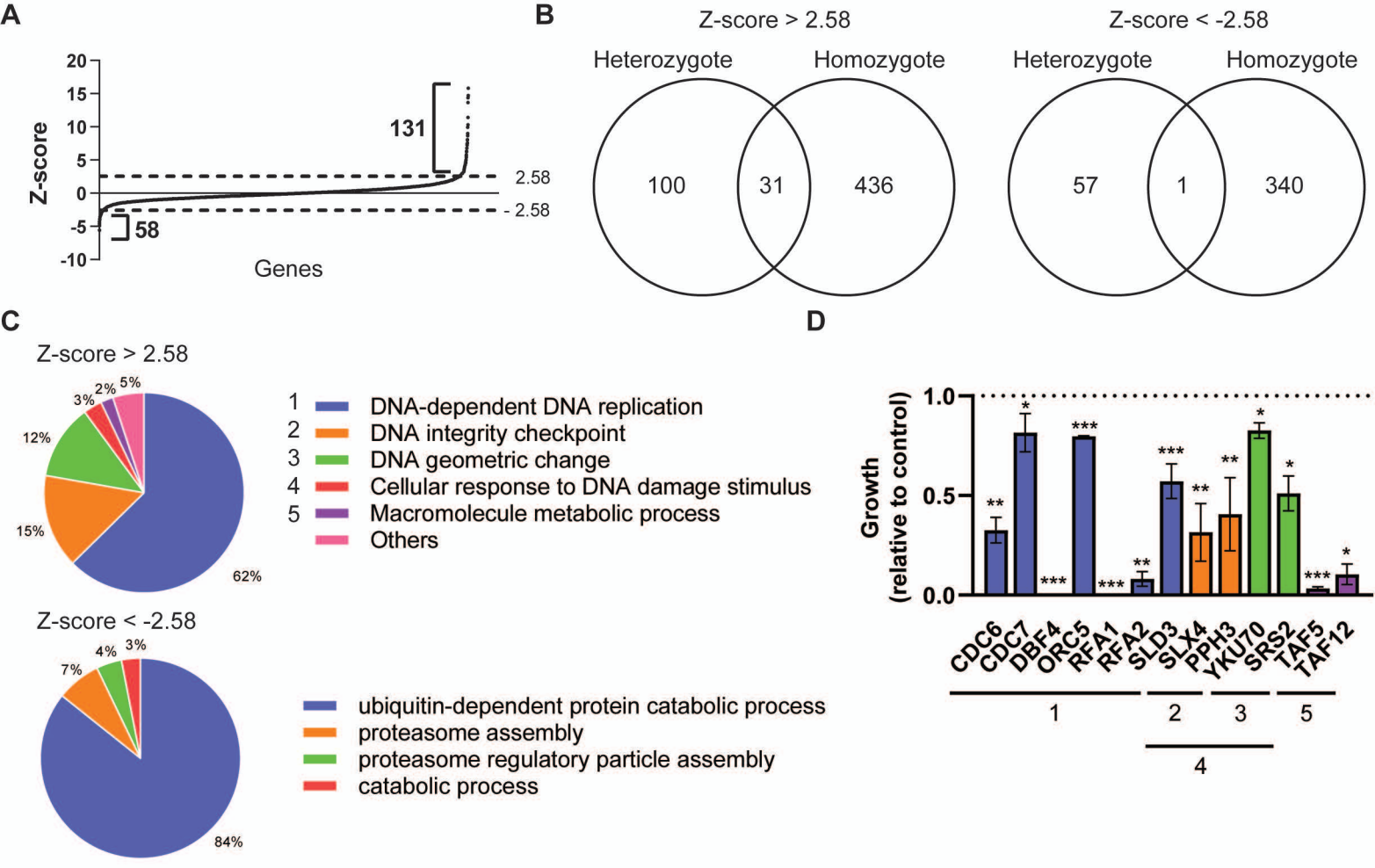
A
Z-score
20
15
10
5
0
-5
-10
131
58
2.58
- 2.58
Genes
B
Z-score > 2.58
Heterozygote
Homozygote
100
31
436
Z-score < -2.58
Heterozygote
Homozygote
57
1
340
C
Z-score > 2.58
62%
15%
12%
3%
2%
5%
1 DNA-dependent DNA replication
2 DNA integrity checkpoint
3 DNA geometric change
4 Cellular response to DNA damage stimulus
5 Macromolecule metabolic process
Others
Z-score < -2.58
84%
7%
4%
3%
ubiquitin-dependent protein catabolic process
proteasome assembly
proteasome regulatory particle assembly
catabolic process
D
Growth (relative to control)
1.0
0.5
0.0
CDC6
CDC7
DBF4
ORC5
RFA1
RFA2
SLD3
SLX4
PPH3
YKU70
SRS2
TAF5
TAF12
1
2
3
5
4

FIGURE 1

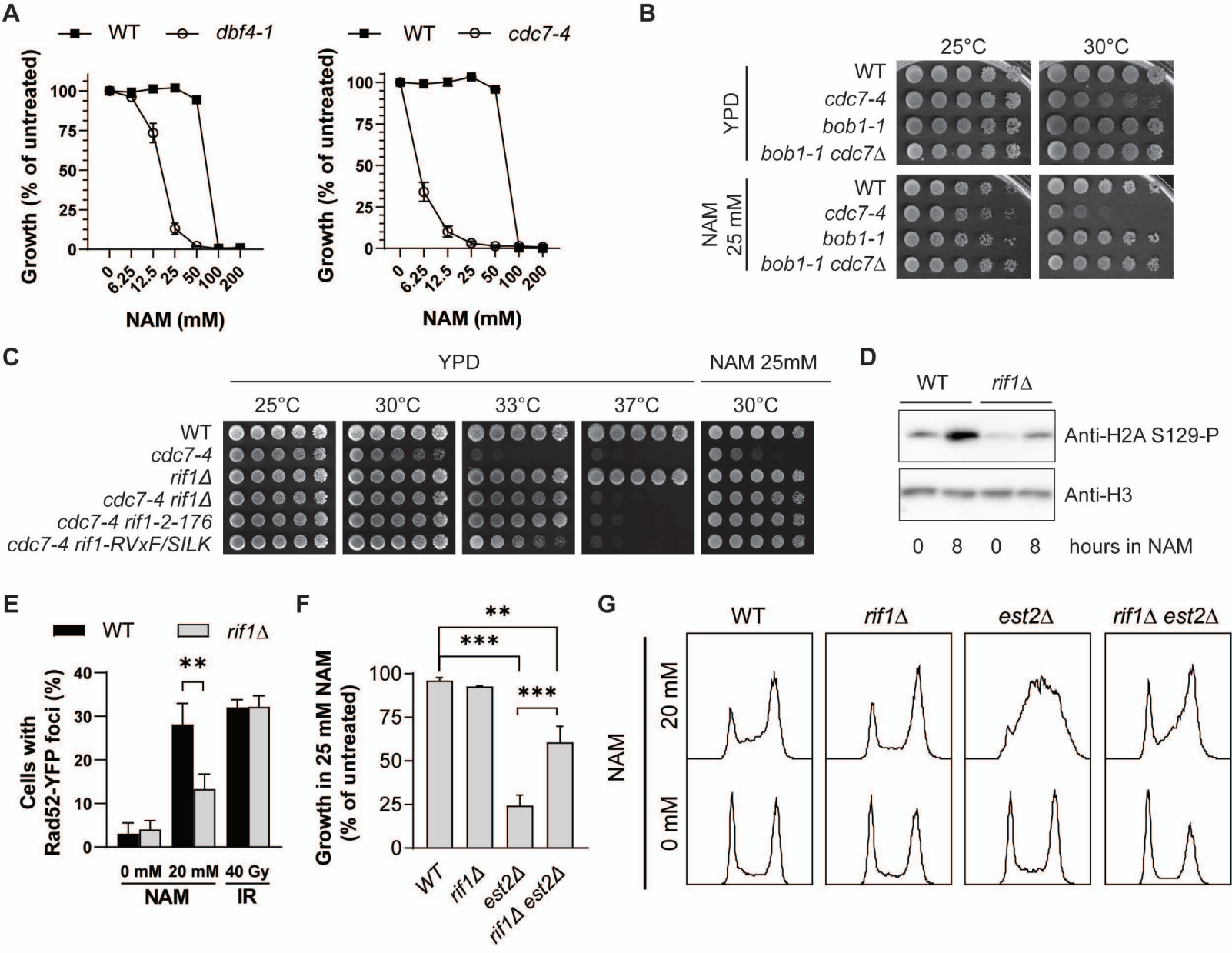
A
WT
dbf4-1
Growth (% of untreated)
100
75
50
25
0
0
6.25
12.5
25
50
100
200
NAM (mM)
WT
cdc7-4
Growth (% of untreated)
NAM (mM)
B
25°C
30°C
YPD
WT
cdc7-4
bob1-1
bob1-1 cdc7Δ
NAM 25 mM
WT
cdc7-4
bob1-1
bob1-1 cdc7Δ
C
YPD
NAM 25mM
25°C
30°C
33°C
37°C
30°C
WT
cdc7-4
rif1Δ
cdc7-4 rif1Δ
cdc7-4 rif1-2-176
cdc7-4 rif1-RVxF/SILK
D
WT
rif1Δ
Anti-H2A S129-P
Anti-H3
0
8
0
8
hours in NAM
E
WT
rif1Δ
Cells with Rad52-YFP foci (%)
40
30
20
10
0
**
0 mM
20 mM
40 Gy
NAM
IR
F
**
***
***
Growth in 25 mM NAM (% of untreated)
100
75
50
25
0
WT
rif1Δ
est2Δ
rif1Δ est2Δ
G
WT
rif1Δ
est2Δ
rif1Δ est2Δ
NAM
20 mM
0 mM

FIGURE 2

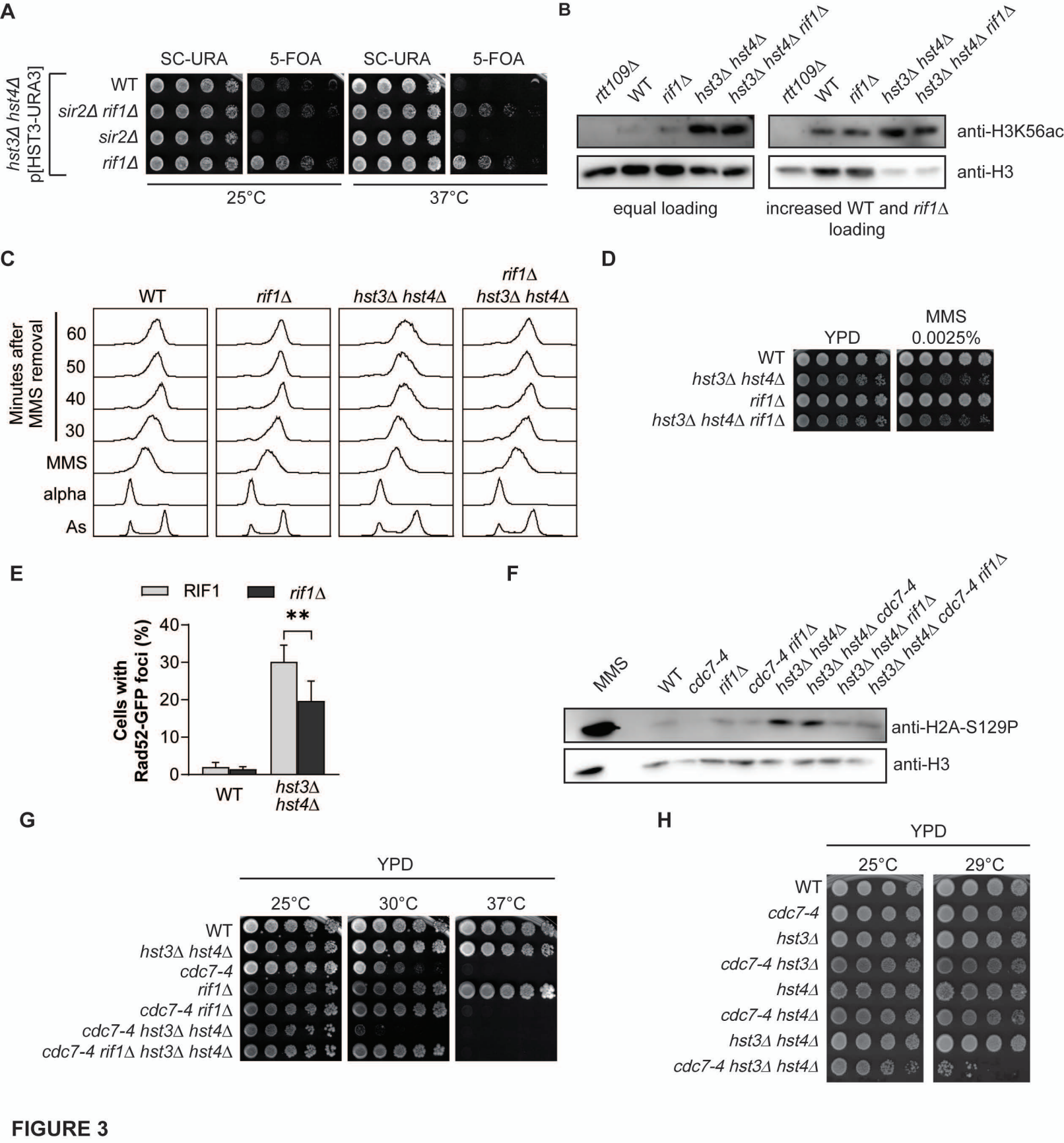
A
hst3Δ hst4Δ p[HST3-URA3]
SC-URA
5-FOA
SC-URA
5-FOA
WT
sir2Δ rif1Δ
sir2Δ
rif1Δ
25°C
37°C
B
rtt109Δ
WT
rif1Δ
hst3Δ hst4Δ
hst3Δ hst4Δ rif1Δ
anti-H3K56ac
anti-H3
equal loading
increased WT and rif1Δ loading
C
WT
rif1Δ
hst3Δ hst4Δ
rif1Δ hst3Δ hst4Δ
Minutes after MMS removal
60
50
40
30
MMS
alpha
As
D
YPD
MMS 0.0025%
WT
hst3Δ hst4Δ
rif1Δ
hst3Δ hst4Δ rif1Δ
E
RIF1
rif1Δ
**
Cells with Rad52-GFP foci (%)
40
30
20
10
0
WT
hst3Δ hst4Δ
F
MMS
WT
cdc7-4
rif1Δ
cdc7-4 rif1Δ
hst3Δ hst4Δ
hst3Δ hst4Δ cdc7-4
hst3Δ hst4Δ rif1Δ
hst3Δ hst4Δ cdc7-4 rif1Δ
anti-H2A-S129P
anti-H3
G
YPD
25°C
30°C
37°C
WT
hst3Δ hst4Δ
cdc7-4
rif1Δ
cdc7-4 rif1Δ
cdc7-4 hst3Δ hst4Δ
cdc7-4 rif1Δ hst3Δ hst4Δ
H
YPD
25°C
29°C
WT
cdc7-4
hst3Δ
cdc7-4 hst3Δ
hst4Δ
cdc7-4 hst4Δ
hst3Δ hst4Δ
cdc7-4 hst3Δ hst4Δ

FIGURE 3

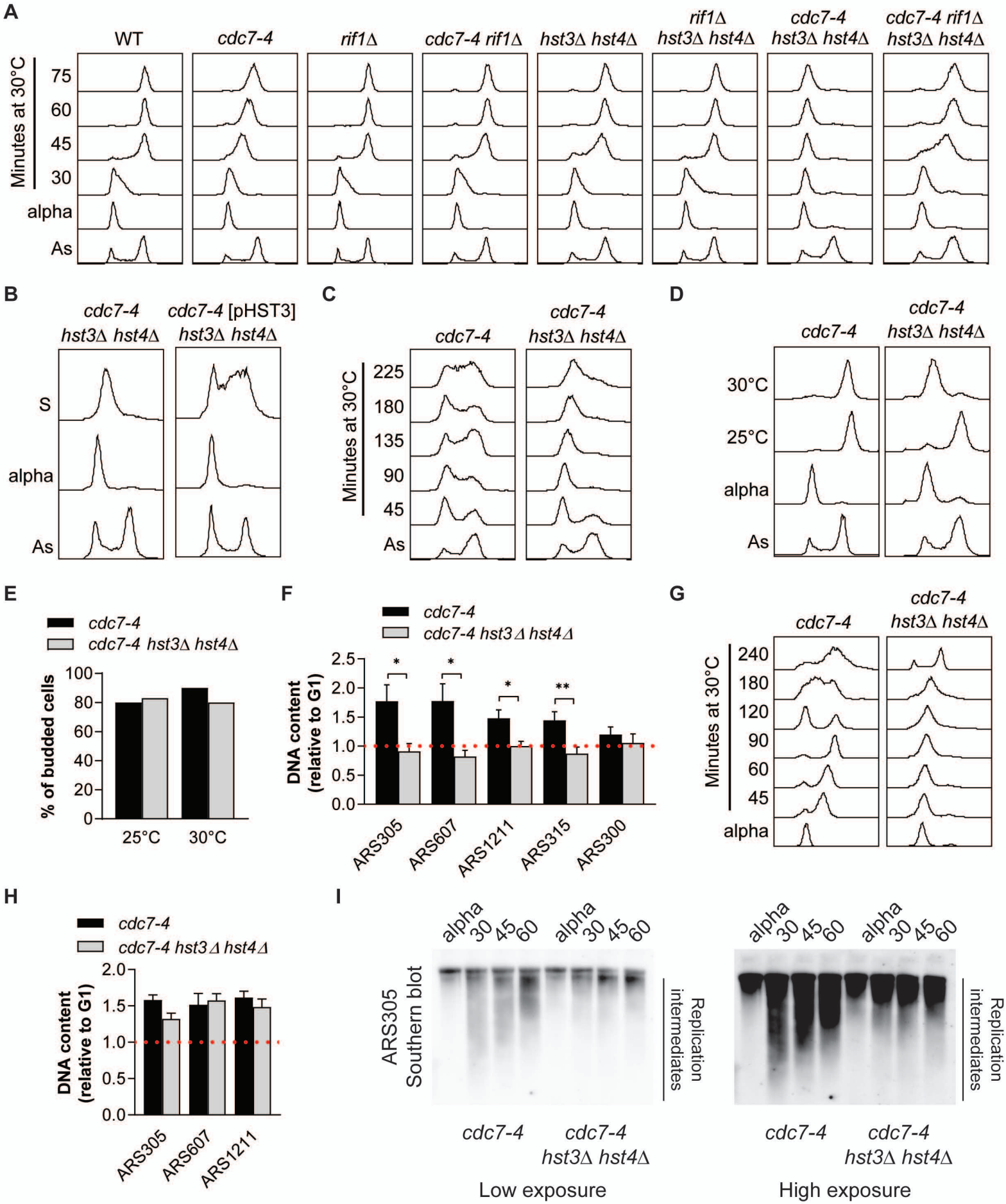
A
WT
cdc7-4
rif1Δ
cdc7-4 rif1Δ
hst3Δ hst4Δ
rif1Δ hst3Δ hst4Δ
cdc7-4 hst3Δ hst4Δ
cdc7-4 rif1Δ hst3Δ hst4Δ
Minutes at 30°C
75
60
45
30
alpha
As
B
cdc7-4 hst3Δ hst4Δ
cdc7-4 [pHST3] hst3Δ hst4Δ
S
alpha
As
C
cdc7-4
cdc7-4 hst3Δ hst4Δ
Minutes at 30°C
225
180
135
90
45
As
D
cdc7-4
cdc7-4 hst3Δ hst4Δ
30°C
25°C
alpha
As
E
cdc7-4
cdc7-4 hst3Δ hst4Δ
% of budded cells
100
80
60
40
20
0
25°C
30°C
F
cdc7-4
cdc7-4 hst3Δ hst4Δ
DNA content (relative to G1)
2.5
2.0
1.5
1.0
0.5
0.0
*
*
*
**
ARS305
ARS607
ARS1211
ARS315
ARS300
G
cdc7-4
cdc7-4 hst3Δ hst4Δ
Minutes at 30°C
240
180
120
90
60
45
alpha
H
cdc7-4
cdc7-4 hst3Δ hst4Δ
DNA content (relative to G1)
2.0
1.5
1.0
0.5
0.0
ARS305
ARS607
ARS1211
I
alpha
30
45
60
alpha
30
45
60
ARS305 Southern blot
Replication intermediates
cdc7-4
cdc7-4 hst3Δ hst4Δ
Low exposure
High exposure

FIGURE 4

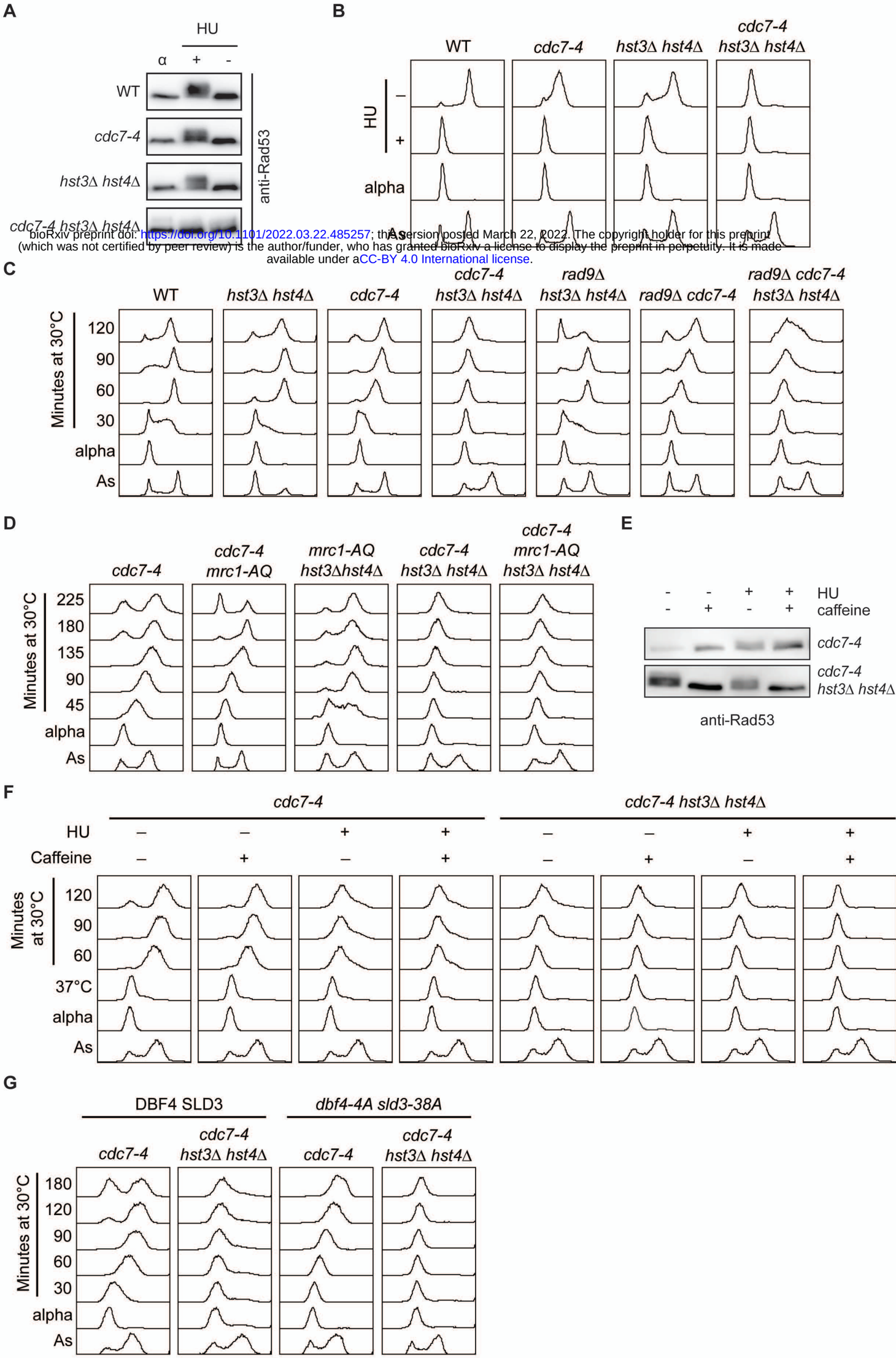

FIGURE 5

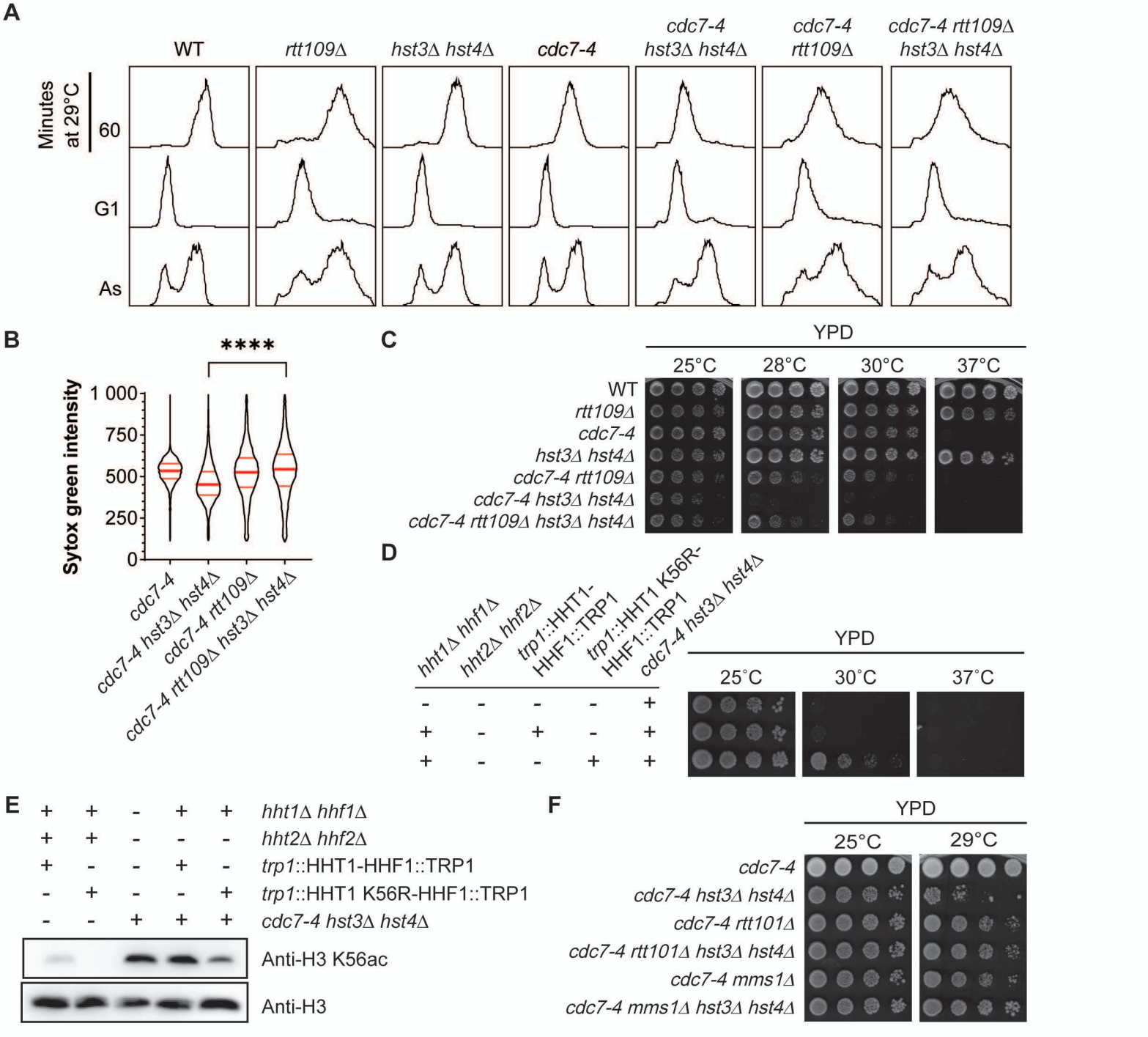
A
WT
rtt109Δ
hst3Δ hst4Δ
cdc7-4
cdc7-4 hst3Δ hst4Δ
cdc7-4 rtt109Δ
cdc7-4 rtt109Δ hst3Δ hst4Δ
Minutes at 29°C
60
G1
As
B
****
Sytox green intensity
1 000
750
500
250
0
cdc7-4
cdc7-4 hst3Δ hst4Δ
cdc7-4 rtt109Δ
cdc7-4 rtt109Δ hst3Δ hst4Δ
C
YPD
25°C
28°C
30°C
37°C
WT
rtt109Δ
cdc7-4
hst3Δ hst4Δ
cdc7-4 rtt109Δ
cdc7-4 hst3Δ hst4Δ
cdc7-4 rtt109Δ hst3Δ hst4Δ
D
hht1Δ hhf1Δ
hht2Δ hhf2Δ
trp1::HHT1-HHF1::TRP1
trp1::HHT1 K56R-HHF1::TRP1
cdc7-4 hst3Δ hst4Δ
YPD
25˚C
30˚C
37˚C
E
hht1Δ hhf1Δ
hht2Δ hhf2Δ
trp1::HHT1-HHF1::TRP1
trp1::HHT1 K56R-HHF1::TRP1
cdc7-4 hst3Δ hst4Δ
Anti-H3 K56ac
Anti-H3
F
YPD
25°C
29°C
cdc7-4
cdc7-4 hst3Δ hst4Δ
cdc7-4 rtt101Δ
cdc7-4 rtt101Δ hst3Δ hst4Δ
cdc7-4 mms1Δ
cdc7-4 mms1Δ hst3Δ hst4Δ

FIGURE 6